DYNAMICS OF LIQUID-SOLID FLUIDIZED BED EXPANSION

by

JAMES ALBERT SCHMITZ

B. S., Kansas State University, 1959

A MASTER'S THESIS

submitted in partial fulfillment of the

requirements for the degree

MASTER OF SCIENCE

Department of Chemical Engineering

KANSAS STATE UNIVERSITY
Manhattan, Kansas

1962

TABLE OF CONTENTS

INTRODUCTION

The term fluidization is used to describe a suspension of solid particles in a fluid flowing through a container. This combination of particles and fluid constitute a fluidized bed. Within this general concept of fluidization there are many special cases which arise. First, the fluid employed may either be liquid or gaseous. Each of these present individual problems of analysis. The solid being fluidized might either be more dense or less dense than the fluidizing fluid. This first case would give rise to the familiar situation of the fluidizing medium, flowing upward through the bed. The latter case would envolve a downward flow of fluid and has never been treated to the author's knowledge. Two distinct mechanisms of fluidization have been defined. First, there is particulate fluidization in which each solid particle is considered to act as an individual unit within the bed. Then there is aggregative fluidization in which the particles are not considered as individual units but as part of groups or aggregates. The distinction between aggregative and particulate fluidization was first observed by Wilhelm and Kwauk (1). Particulate fluidization is characterized by the existence of a homogeneous particle distribution, while in aggregative fluidization, two phases, dilute and dense, are seen to exist. Finally, the geometry of the container may be chosen at will. Most of the work to date has been carried out in columns with circular cross sections, but there have been a few studies made using columns with square cross sections.

This work is concerned with the fluidization of spherical, solid particles by a liquid of less density in a column of circular cross section. The very nature of the experimental and analytical work envolved imply that the fluidization is to be particulate or very nearly particulate.

The use of fluidization in industry is very wide and is increasing in scope (2). A few of the more important applications are summarized as follows:

1) Chemical reactors.
   a) Where the fluid stream is composed of the reacting component and the solid particles catalyze the reaction.
   b) Where reaction takes place between the fluid and solid.
2) Mass transfer operations.
   a) Leaching.
   b) Adsorption.
   c) Drying.
3) Evaporation.
   a) Solid particles can be fluidized in a boiler to prevent scale formation on heat transfer surfaces.
4) Nuclear reactors.
   a) Fluid acting as moderator and particles as fuel elements.
   b) Fluid acting as fuel element and particles as moderator.

5) Elutriation or separation of particles by their different fluidizing characteristics.

6) Calcination and heat treatment processes.

Generally the fluidization technique will yield relatively high heat and mass transfer coefficients and will provide a high degree of mixing between fluid and particles.

Process Control Considerations

In many of the applications summarized the maintenance of a given porosity or bed height is either desirable or essential. For instance, the neutron density of a fluidized nuclear reactor will be a function of porosity, and failure to maintain a given porosity within certain limits will result in a non-critical condition. Also in any application of fluidization there will be a porosity determined by design procedures or by experimental work at which the process is to operate. Therefore, the problem of process control is becoming increasingly apparent in the area of fluidization as in all phases of the chemical process industry. In the past, a large portion of process control has been accomplished by human operators directly observing the process and making necessary corrections. At the present time the need for products of higher quality and the high speed response of equipment have rendered the human approach to control impractical. Financial considerations also dictate a need for automatic control of processes. Ceaglske (3) defines automatic control as follows:

"A control system consists of a series of units combined to produce a desired effect with little or no human supervision.

The basic parts of the system are the process, the measuring element, the error-detecting mechanism, the controller, and the final control element."

The measuring element continuously measures the value of some process variable and sends a signal which is proportional to the measured variable to the error-detecting mechanism. The error-detecting mechanism then compares the value of the measured variable with the desired value and indicates this difference, or error, to the controller. The controller takes corrective action based on the error signal and indicates to the final control element the necessary change to be effected in the input variable. Therefore, the system consists of a closed circuit in which the input at any time is dependent upon the output at a time just preceding.

The nature of the corrective action taken depends upon the type of controller employed. A proportional controller is one which dictates a corrective action proportional to the error detected. The integral controller acts upon the integral of the error with time. Likewise, there are rate dependent and two-position controller as well as combinations of these various modes.

Each of the elements of a control system has its own response characteristics, and the performance of the system as a whole is dependent upon a combination of the various individual characteristics. It is therefore necessary for the system designer to have at his disposal information on the dynamic characteristics of each component of the system. By far the most important component is the process itself since the design of all the other components is dependent on the dynamic behavior of this element.

The disturbances a process may experience are usually random in nature, and it is very difficult to determine the response of the system to random inputs. However, it is possible to describe the response of a system to any input as a combination of its responses to certain regular inputs. In particular the transient response to a step input and the steady-state response to a sinusoidal input are useful.

In analyzing the dynamic characteristics of a system one of two methods is generally used. The first involves the derivation of a differential equation describing the process and solving it for the desired inputs to obtain response characteristics. This method is quite convenient when the differential equation admits an analytical solution in closed form. However, when the equation requires solution by series or numerical methods, the solution obtained is not nearly as useful for control system design. A relatively new and very powerful method of system analysis involves the use of analog computers. Use of this method requires only that a differential equation describing the process be available. Electrical circuits in the analog are set up according to the equation, and the analog computer than simulates the process. Any input can be fed into the computer and the response noted. This information is then used in the design of the actual control system. This method of analysis is particularly useful in the analysis of non-linear systems.

The fluidized bed presents a typical non-linear problem. The non-linear element existing in fluidized bed analysis can be considered roughly analogous to the non-linearities occuring in heat and mass transfer. Just as the heat and mass transfer coeffi-

cients are dependent upon the fluid flow conditions, the relationship between fluidizing velocity and porosity is also dependent on flow conditions. Although quite a bit of work has been done on the analysis of the dynamic behavior of heat and mass transfer equipment, little has been done on the fluidized bed expansion.

Purpose

The major purpose of this work was to develop a linearized model to describe the dynamic behavior of the liquid-solid fluidized bed and to verify that model with experimental results. It was hoped that a sufficiently accurate representation could be obtained to be useful in the design of control systems for fluidization processes.

EXPERIMENTAL

Apparatus and Equipment

Photographes of the equipment are shown in Figs. 1 and 2 and a schematic diagram is shown in Fig. 3.

The column used was a 24-inch high, 1.982-inch diameter glass column. The column was seated on a piece of 3/4-inch Lucite with a 2-inch diameter hole through the center. A circular piece of U. S. Standard 200 mesh screen was glued in the center of the Lucite slab. A piece of U. S. Standard 30 mesh screen was glued directly under the 200 mesh in order to provide support. This screen assembly formed the bottom boundary for the bed and also provided a degree of mixing or distribution for the fluidizing

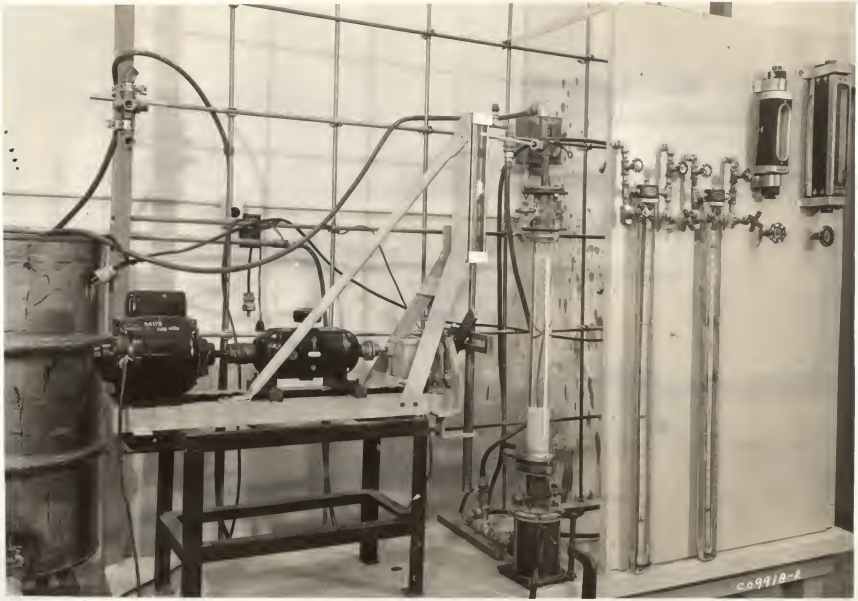

Fig. 1. Front view of experimental apparatus.

Fig. 2. Side view of experimental apparatus.

A	Constant head tank	F	Column
B	Pump	G	Thermometer
C	Solenoid valves	H	Rotameter
D	Calming section	I	Sine-wave generator
E	Screen	J	Overflow pipe

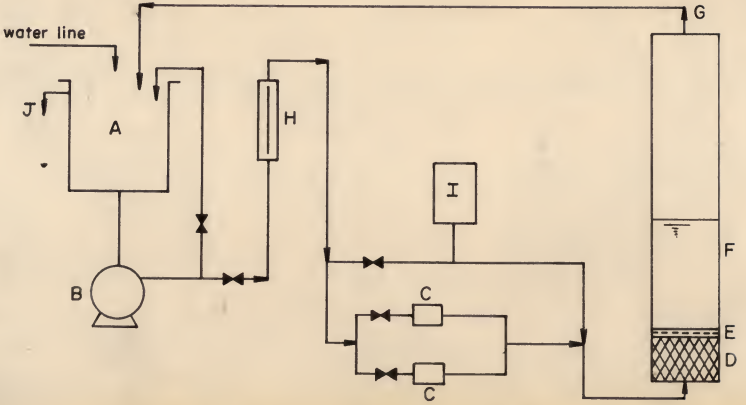

Fig. 3. Diagram of experimental apparatus

stream. The column and its accessories sat directly over a calming section. The bottom portion of the calming section was six inches high and had an inside diameter of four inches. The top portion which was connected to the Lucite screen supporter was 3 1/2 inches high with a two inch inside diameter. The calming section was packed with 1/4-inch Berl saddles to such a height that the top of the packing was 1/8- to 1/4-inch below the supporting screens. This packed region was used for the purpose of providing a more or less flat velocity profile at the entrance of the column. The fluid entered the calming section through a pipe welded in its side at the bottom. At the top of the column another 200 mesh screen was held in place between two rubber gaskets. This prevented any of the smaller particles from being carried out of the column and through the system. Immediately above this screen a short section of two inch pipe was placed. This pipe was equipped with a temperature well, thus providing a means of reading the temperatures of the liquid just as it left the bed. The water supply was a 50 gallon constant-head tank. Water which had circulated through the system was returned from the top of the column back to the supply tank. The only problem encountered in this scheme was the slight rise in temperature the water experienced upon flowing through the system. Since the experimental work was to be conducted under isothermal conditions, it was necessary to continually add a small flow of tap water to the supply tank and let the excess overflow through a pipe. This procedure worked out very well and it was possible to maintain a constant temperature within $\pm$ 1°F. The water was forced through

the system by means of an Eastern, Model F, pump. The flow through the system was measured by means of two rotameters in parallel. Only one of these rotameters was utilized for any one experiment. The choice depended on the desired range of flow rates. Calibration curves for the two rotameters are shown in Figures 4-(a) and 4-(b).

When it was desired to produce a step or pulse input in flow rate, the flow was directed through a circuit consisting of two solenoid valves in parallel. Each of these valves was in series with a globe valve which could be used to regulate the flow through that particular line when it was open. The solenoids used were Sporlan, Type 12 P and were 3/8 inch, two-way valves. They were connected through one electrical switch in such a manner that one would be open and the other closed on each switch position.

Sine-wave generator: The apparatus used for producing a sine or cosine input in fluidizing velocity consisted of five main units:

(1) Power for the apparatus was supplied by a General Electric, 1/2 h.p., Model 5KC63AB66B, A.C., motor operating at 1725 R.P.M.

(2) The output from the motor drove a Vickers 3/4 h.p. hydraulic transmission, Model No. TR3-HR13-F18-13, with a maximum input and output speed of 1800 R.P.M. This was a variable speed transmission giving an output ranging from 0 to 100% of the input speed.

(3) The output from the Vickers transmission was further re-

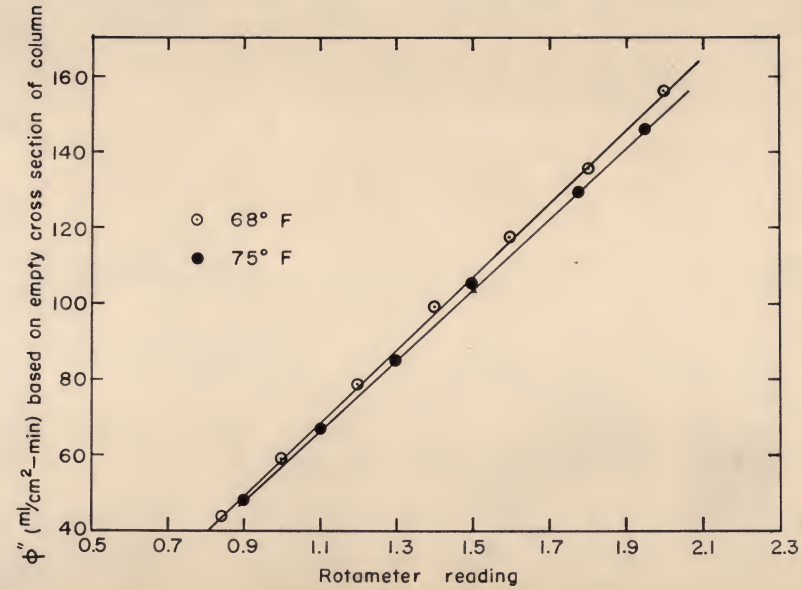

Fig. 4–(a). Calibration of rotameter 52.

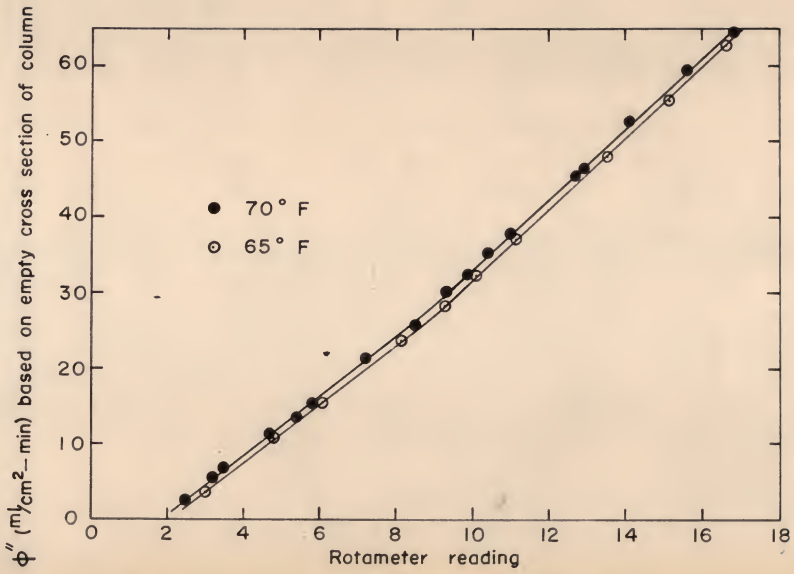

Fig. 4–(b). Calibration of rotameter 23.

duced by use of a 200-1 reduction gear assembly. This was necessary due to erratic performance of the hydraulic transmission at the very low frequencies desired.

(4) The conversion from the constant speed rotational output from the gear assembly to longitudinal motion with a sine varying velocity was accomplished using the apparatus described in Fig. 5. The lever arm shown was equipped with drilled and tapped holes at 1/4 inch intervals, thus providing lengths from 1-1/2 inches to 5-3/4 inches.

(5) The final unit was a Model 24 Alkon Cylinder with a 12 inch maximum stroke. The diameter of this cylinder was 1-3/4 inches.

A photograph of the sine-wave generator is shown in Figure 6.

Particles

Five different groups of particles were employed in this experiment. The particle size range within each group and the particle density were as follows:

(I) These particles were Propper Borosilicate size 3 beads, 6 to 7 U.S.-mesh. Particle diameters ranged from 2.83 mm. to 3.36 mm; the average diameter was 2.87 mm. As is evident by observing the average diameter in comparison with the two extremes, the size distribution was not normal. In fact, 25 of these particles were measured with a micrometer giving an average of 2.87 mm. and a variance of only $2.37 \times 10^{-4} mm^2$. The density of the particles was 2.5 g./cc.

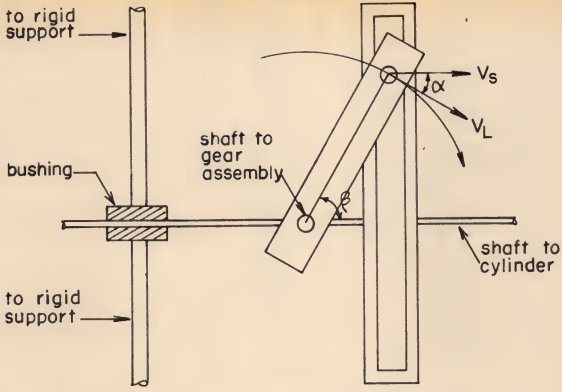

Let V_S = Velocity of shaft to cylinder

V_L = Tangential velocity of lever arm

α = Angle between V_S and V_L

β = Angle between lever arm and shaft to cylinder

Then, $V_S = V_L \cos \alpha$

$\beta = 90° - \alpha$

$\therefore$ $V_S = V_L \sin \beta$

Since the cross-sectional area of the cylinder is constant the flow rate produced by a constant rotational velocity, V_L, is

$$V = A_{cy} V_S = A_{cy} V_L \sin \beta$$

Where V = Volumetric flow rate (ml/sec)

A_{cy} = Cross sectional area of cylinder (cm^2)

Fig. 5. Assembly for sine-wave production.

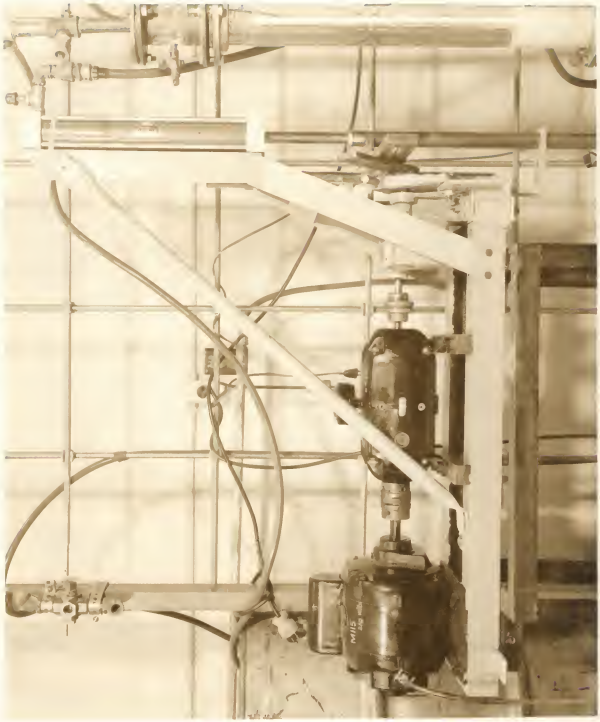

Fig. 6. Photograph of sine-wave generator.

(II) These particles were Nalcite ion exchange resin manufactured by the Nalco Chemical Company. The particles were screened and the 25 to 30 U.S.-mesh fraction used, giving a particle diameter range of 0.59 mm. to 0.71 mm. Since this material absorbs a considerable amount of water, all screening and physical property estimation were conducted with the particles saturated with water. The density of the particles was 1.08 g./cc.

(III) These particles as well as those in particle groups IV and V were glass beads manufactured by the Minnesota Mining and Manufacturing Company. This group consisted of the 40 to 45 U.S.-mesh fraction giving a particle diameter range of 0.35 mm. to 0.42 mm. The density of these particles was 2.5 g./cc.

(IV) These particles were identical to those of group III with the exception that they were the 60 to 70 U.S.-mesh fraction giving a particle diameter range of 0.21 mm. to 0.25 mm.

(V) These particles were identical to those of groups III and IV with the exception that they were the 70 to 80 U.S.-mesh fraction giving a particle diameter range of 0.177 mm. to 0.21 mm.

Henceforth, these particle groups will be specified by their U. S. mesh range.

The close cuts in particle size range were considered necessary in order to minimize the effect of size distribution. Another aspect which must be considered is the sphericity of the particles.

In all cases the particles are considered spherical and the following evidence is given for this assumption. In group I, the particles were large enough to permit measurement by micrometer. Therefore several of these particles were measured along different axes to obtain an indication of their symmetry. The following data are representative of these measurements:

Table 1. Measurement of particles in Group I for symmetry.

Particle No.	Diameter (inches)
1	0.1132
"	0.1129
"	0.1133
"	0.1137
2	0.1113
"	0.1129
"	0.1110
"	0.1128
3	0.1163
"	0.1168
"	0.1148
"	0.1158

The particles in the other groups were too small to allow individual measurement. In this case an indication was obtained by comparing the values of terminal falling velocity observed experimentally with those calculated assuming spherical particles. These figures are presented in Table 2.

Table 2. Terminal velocities of particles.

Particle Group No.	U_s (calculated) (cm./sec.)	U_s (experimental) (cm./sec.)
II	1.00	1.15
III	4.82	5.06
IV	2.68	2.83
V	2.12	2.35

It can be seen that in all cases there is fair agreement, and while this analysis does not provide a quantitative prediction of sphericity, it does indicate that the particles have a sphericity close to 1.0.

Procedure

General: The desired weight of particles of a particular group were placed in the column. The temperature of the fluidizing water was fixed and maintained at some constant value. Steady state fluidization data were then obtained by setting the flow rate at a constant value, allowing a sufficient amount of time for the bed to reach equilibrium, and reading the rotameter and bed height. All bed height readings were made using a scale calibrated in centimeters which was pasted on the side of the column. This was repeated for various bed expansions and the results recorded.

Step Change Data: The bed was allowed to come to and remain at some steady-state height. A switch was thrown which caused both solenoid valves to operate and effect a change in flow from one line to the other, giving a step change in flow rate to the

bed. The instantaneous bed height was read at regular time intervals during the transition from the initial steady-state height to the final steady-state height.

Pulse Data: The response to a pulse composed of two step inputs was obtained in much the same manner as the response to a step change. The only difference in procedure was to effect a second step change in flow back to the original flow rate at some time before the bed height reached the steady-state value corresponding to the intermediate flow rate.

Frequency Response Data: A steady state flow rate was first set and the bed allowed to come to equilibrium. The sine wave generator was adjusted for lever arm length and rotational velocity in order to obtain the desired input amplitude and frequency. The sine input was then superimposed on the steady-state flow rate. After waiting a few cycles to insure that the transient effects had sufficiently subsided, the maximum and minimum in bed height were read and recorded. Phase lag data were obtained by observing and recording the time difference between the reversal in piston direction and the reversal in bed direction. This was not possible when operating at high frequencies where the phase lag was close to 90° and the time interval between reversals was very small.

Effect of Load Changes on Steady State Fluidizing Velocity

One question which might arise pertaining to the experimental procedure is the effect of the transient flow producing elements

of the system on the performance of the supply pump and therefore on the steady-state flow delivered. Figure 3 shows that these elements are directly connected to the steady-state circuit.

In particulate fluidization the pressure drop through the bed is very nearly independent of flow rate or bed heigth. Therefore, for the step input, the only change in load is due to increased friction losses in the lines. It is assumed that this effect is almost instantaneous so that little distortion of the input occurs. For the sine wave input the situation is quite different. The sine generator is imposing a continually changing load on the system and it might be expected that some of its effect would be transmitted back through the system causing the steady-state flow to vary. It would, however, be possible to detect any such effect by observing the rotameter. No oscillating of the rotameter was observed during any of the experiments, thus confirming that a valid steady-state flow was being obtained. This was evidently due to the fact that the load changes were small and that the pump was operating on a fairly level portion of its' load-output curve. At sinusoidal inputs of greater amplitude than were necessary in this experiment, oscillations were observed in the steady-state flow and this is definitely a problem in any experimentation of this nature.

DEVELOPMENT OF LINEARIZED MATHEMATICAL MODEL

As was stated in the introduction, the major analytical tool used in this work was a linearized description of the basically non-linear process.

Richardson and Zaki (4) showed that for steady-state behavior the porosity can be related to the fluidizing velocity by

$$\phi_{ss} = U_s \epsilon_{ss}^n \tag{1}$$

where ϕ_{ss} is the steady-state superficial liquid velocity, U_s is the terminal falling velocity of the particle, ϵ_{ss} is the steady-state porosity, and n is a constant characteristic of the particle-liquid system.

In considering the response of a liquid-solid fluidized bed to a step-input in fluidizing velocity, Slis, et. al. (5) extended Equation (1) to the unsteady-state case and obtained the following expression for the rate of change of the bed height:

$$\frac{dh}{dt} = \phi_1 - U_s \epsilon_h \tag{2}$$

where h is the instantaneous bed height, t is the time, ϕ_1 is the superficial liquid velocity after the step input, and ϵ_h is the instantaneous porosity at the top of the bed.

For the steady-state case, $dh/dt = 0$, $\phi_1 = \phi_{ss}$, and Equation (2) reduces to Equation (1).

Equation (2) can be linearized by letting

$$\phi_1 = \phi_{ss} + \Delta\phi \tag{3}$$

$$h = h_{ss} + \Delta h \tag{4}$$

$$\epsilon_h = \epsilon_{ss} + \Delta\epsilon \tag{5}$$

Now ϵ_h^n can be expanded in a Taylor series about ϵ_{ss} to give

$$\epsilon_h^n = \epsilon_{ss}^n + n\,\epsilon_{ss}^{n-1}\Delta\epsilon + \cdots \tag{6}$$

Substitution of Equations (3), (4) and (6) into Equation (2) gives

$$\frac{dh_{ss}}{dt} + \frac{d(\Delta h)}{dt} = \phi_{ss} + \Delta\phi - U_s\epsilon_{ss}^n + n\,\epsilon_{ss}^{n-1}\Delta\epsilon \tag{7}$$

Since the amount of solids in the bed remains constant, an instantaneous material balance is written as

$$(1-\epsilon)h = (1-\epsilon_{ss})h_{ss} \tag{8}$$

where ϵ is the instantaneous porosity.

Differentiation of Equation (8) gives

$$\frac{d\epsilon}{dh} = \frac{(1-\epsilon_{ss})h_{ss}}{h^2} \tag{9}$$

for small changes in h, Equation (9) becomes

$$\Delta\epsilon = \left(\frac{1-\epsilon_{ss}}{h_{ss}}\right)\Delta h \tag{10}$$

Substituting Equation (10) into Equation (7) gives

$$\frac{d(h_{ss})}{dt} + \frac{d(\Delta h)}{dt} = \phi_{ss} + \Delta\phi - U_s\epsilon_{ss}^n - U_s\, n\,\epsilon_{ss}^{n-1}\left(\frac{1-\epsilon_{ss}}{h_{ss}}\right)\Delta h$$

but $$\frac{dh_{ss}}{dt} = 0 = \phi_{ss} - U_s\,\epsilon_{ss}^n \tag{11}$$

and consequently Equation (11) reduces to

$$\frac{d(\Delta h)}{dt} + \frac{1}{\dfrac{h_{ss}}{U_s\, n\, \epsilon_{ss}^{n-1}\,(1-\epsilon_{ss})}}\,\Delta h = \Delta\phi \qquad (12)$$

ϕ can be arbitrarily written as

$$\frac{1}{\dfrac{h_{ss}}{U_s\, n\, \epsilon_{ss}^{n-1}\,(1-\epsilon_{ss})}}\,A_i \equiv \Delta\phi \qquad (13)$$

Substitution of Equation (13) into Equation (12) and a change of dependent variable from Δh to h gives

$$\frac{dh}{dt} + \frac{1}{\dfrac{h_{ss}}{U_s\, n\, \epsilon_{ss}^{n-1}\,(1-\epsilon_{ss})}}\,h = \frac{A_i}{\dfrac{h_{ss}}{U_s\, n\, \epsilon_{ss}^{n-1}\,(1-\epsilon_{ss})}} \qquad (14)$$

If we consider the liquid-solid fluidized bed to be a first order (time constant) system, the rate of change of height can be written as

$$\frac{dh}{dt} + \frac{1}{T}h = \frac{h_i}{T} \qquad (15)$$

where T is the time constant for the system and h_i is the input function.

For a step change in fluidizing velocity, the input function, h_i, is a constant, A_i, so that Equation (15) becomes

$$\frac{dh}{dt} + \frac{1}{T}h = \frac{A}{T}i \tag{16}$$

Comparing Equation (14) with Equation (16) shows that the time constant of the system is

$$T_1 = \frac{h_{ss}}{U_s n \epsilon_{ss}^{n-1} (1-\epsilon_{ss})} \tag{17}$$

By substituting Equation (1) into Equation (17), the time constant can also be written as

$$T_2 = \frac{h_{ss} \epsilon_{ss}}{\phi_{ss} n (1-\epsilon_{ss})} \tag{18}$$

Either Equation (17) or Equation (18) can be used to calculate the theoretical time constant of the liquid-solid fluidized bed.

Solutions for Standard Inputs

The solutions of Equation (15) or (16) for various input functions are given below.

Step Input: Integration of Equation (15) or (16) gives, for $A_i = A$ = Step size,

$$-\frac{t}{T} = \ln\left[1 - \left(\frac{h-h_{ss}}{A}\right)\right] \tag{19}$$

or

$$\frac{h-h_{ss}}{A} = 1 - e^{-t/T} \tag{20}$$

as a solution for the step input.

Pulse Input: The input considered here is composed of two step inputs separated by a time interval, a. The second step is of the same magnitude as the first, but opposite in direction. The solution to Equation (15) for this input is

$$\frac{h-h_{ss}}{A} = (1-e^{-t/T}) - u(t-a)\quad e^{-\frac{(t-a)}{T}} \qquad (21)$$

$$(t-a) > 0$$

where u is the unit step function:

$$u(t-a) = 0 \quad \text{for } 0 < t < a$$

$$= 1 \quad \text{for } a < t$$

Ramp Input: The response to a linearly varying input, $h_i = Bt$, is

$$\frac{h-h_{ss}}{A} = BT\,(e^{-t/T} + \frac{t}{T} - 1) \qquad (22)$$

Sinusoidal Input: For the input $h_i = h^* \sin\omega t$, the solution to Equation (15) is

$$\frac{h-h_{ss}}{h^*} = \frac{\sin(\omega t+\alpha)}{\sqrt{1+T^2\omega^2}} \qquad (23)$$

where h^* is the input amplitude in terms of the height variable, ω is the angular frequency, and α is the phase lag.

From Equation (23) it is seen that the amplitude ratio is given

by

$$A.R. = \frac{\text{output amplitude}}{\text{input amplitude}} = \frac{h^* / \sqrt{1+\omega^2 T^2}}{h^*} \qquad (24)$$

$$= \frac{1}{\sqrt{1+\omega^2 T^2}}$$

and the phase lag,

$$\alpha = -\arctan \omega T \qquad (25)$$

ANALYSIS OF DATA

As stated in the experimental section, the experimental data consisted mainly of the measurement of bed height as a function of time under the variable flow rate. Flow rate and properties of the liquid-solid system were also recorded. Data were obtained on the system response to three inputs; step input, pulse input, and sinusoidal input. For analysis the data obtained for each of these inputs will be treated separately.

Response to Step Input

The data taken on the response to a step-input in fluidizing velocity was to be used to verify the linearized model developed in the previous section. Figure 7 shows typical step change response curves.

Referring to Equation (19) it can be seen that a plot of time, t, versus the group $\ln \left[1 - \frac{h-h_{ss}}{A} \right]$ should yield a straight

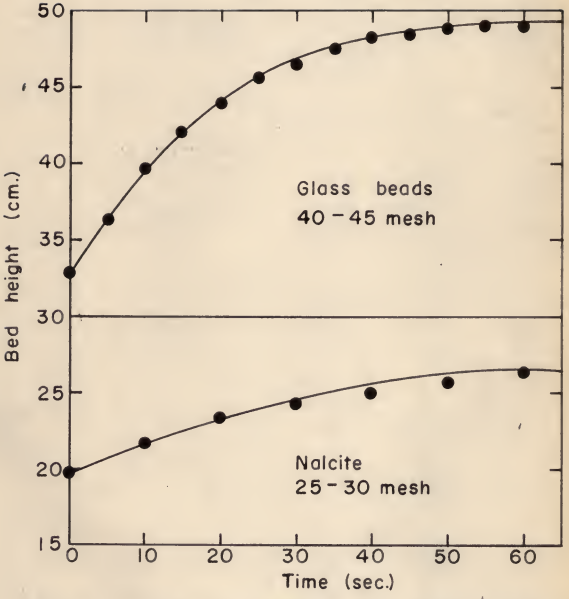

Fig. 7. Time vs. height for step input.

line of slope, 1/T. Therefore, by plotting the experimental data expressed in this form, an experimental determination of the time constant, T, was obtained for each experimental run. A typical determination of the experimental time constant is shown in Figure 8. It should be noted that the time constant is also given by the time corresponding to $\ln \left| 1 - \frac{h-h_{ss}}{A} \right| = -1$. This is immediately apparant from the form of Equation (19). Since the points on Figure 8 fall very nearly on a straight line for the first 35 seconds, there is very little question as to how the straight line is to be drawn. However, for various reasons to be discussed later, the experimental points did not always behave in this manner. When curvature at the origin was observed, the straight line was always drawn so as to represent the tangent to the curve at the origin. This procedure was adopted because of the manner in which the linearized model was developed. When $h = h_{ss}$, $\ln \left[1 - \frac{h-h_{ss}}{A} \right] = 0$, so that the origin represents the point where the model should best represent the response. An instance where this procedure was necessary is shown in Figure 9. The rapid deviation of this curve from the straight line is caused by the fact that the curve represents a response to a step-down in flow rate and this case is not approximated nearly as well as the response to a step-up by the linearized model. It is seen, however, that the approximation is accurate for a short period of time.

In the development of the linearized model the theoretical expression for the time constant was found to be

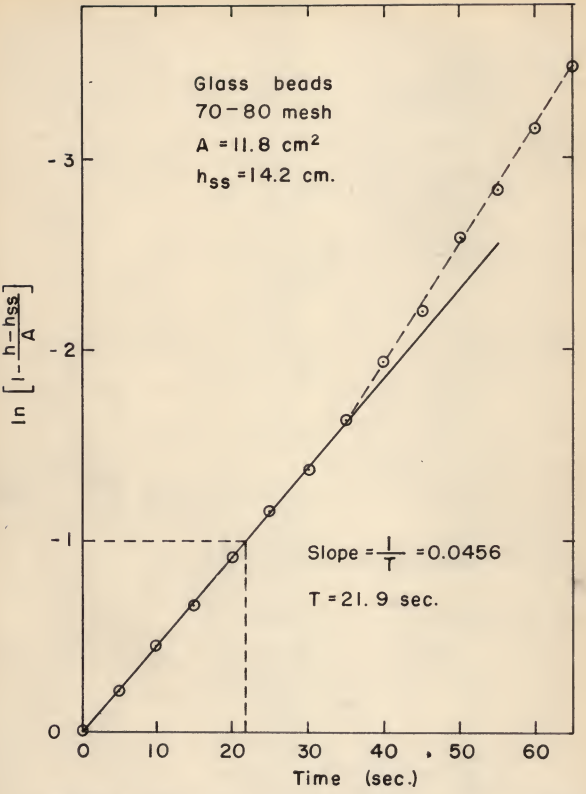

Fig. 8. Experimental determination of time constant.

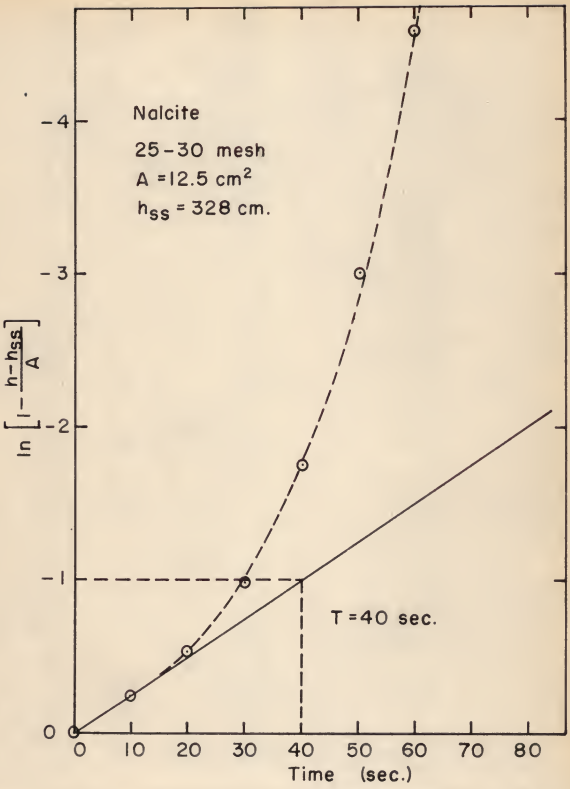

Fig. 9. Experimental determination of time constant.

$$T \quad \frac{h_{ss}}{nU_s \epsilon_{ss}^{n-1} (1-\epsilon_{ss})}$$

The values of h_{ss} and ϵ_{ss} are fixed by the experimental operating conditions and values of U_s were determined experimentally and calculated as discussed in the experimental section. The equations used to calculate U_s were

$$\text{Stokes Law:} \quad U_s = \frac{g_c D_p^2 (\rho_s - \rho_L)}{18} \qquad 0.0001 < N_{Re} < 2.0 \qquad (26)$$

$$\text{Intermediate Law:} \quad U_s = \frac{0.153\, g_c^{0.71} D_p^{1.14} (\rho_s - \rho_L)^{0.71}}{\rho_L^{0.29}\, \mu^{0.43}}$$

$$2.0 < N_{Re} < 500 \qquad (27)$$

where g_c is the gravitational constant, ρ_s is the density of the particles, ρ_L is the density of the liquid, μ is the viscosity of the liquid, and N_{Re} is Reynolds number.

The constant, n, can be calculated by the following equations given by Richardson and Zaki (4).

$$n = 4.65 + 19.5\ d/D \qquad N_{Re} < 0.2 \qquad (28)$$

$$n = (4.34 + 17.5\ d/D)\ N_{Re}^{-0.03} \qquad 0.2 < N_{Re} < 1 \qquad (29)$$

$$n = (4.45 + 18\ d/D)\ N_{Re}^{-0.1} \qquad 1 < N_{Re} < 200 \qquad (30)$$

$$n = 4.45\ N_{Re}^{-0.1} \qquad 200 < N_{Re} < 500 \qquad (31)$$

$$n = 2.39 \qquad 500 < N_{Re}$$

In Table 3 all of the experimentally determined time constants are presented along with those calculated by Equation (17). The percentage deviation of theoretical and calculated time constants was calculated by

$$\%\Delta = \left(\frac{T_{exp} - T_{cal}}{T_{exp}}\right)100 \tag{33}$$

In Table 3 experiments denoted by SU were for a step-up in fluidizing velocity, and those denoted by SD, were for a step-down.

In order to obtain some idea of the applicability of the linearized model, it was necessary to devise an arbitrary test. A time interval, $t_{0.02}$, was defined in such a manner that the expression

$$\left| \left(\frac{h-h_{ss}}{A}\right)_{exp} - \left(\frac{h-h_{ss}}{}\right)_{cal} \right| < 0.02 \tag{34}$$

was valid within the interval. The subscript, exp and cal in expression (34) refer to experimental values and values obtained by the linearized model respectively. The values of $t_{0.02}$ are tabulated for each experimental run in Table 4.

Table 3. Step input analysis.

Exp. No.*	h_{ss}(cm.)	ϵ_{ss}	A(cm.)	T(sec.) exp.	T(sec.) cal.	%Δ
SET I - 70-80 mesh particles, Bed wt. 400 gms. s 2.5 g./cc.						
SU-2	14.14	0.658	10.7	22.2	18.2	18.0
SU-3	14.14	0.658	11.8	21.6	18.2	15.7
SU-4	14.14	0.658	2.3	20.0	18.2	10.1
SD-5	33.44	0.763	19.2	31.5	38.1	-20.9
SD-6	33.44	0.763	19.2	31.8	38.1	-19.8
SET II - 60-70 mesh particles, Bed wt. 400 gms. s 2.5 g./cc.						
SU-7	16.2	0.513	33.5	31.6	30.1	4.7
SU-8	22.8	0.654	6.6	20.5	21.0	-2.4
SU-9	23.6	0.664	8.4	20.9	23.5	-12.5
SU-10	16.1	0.509	7.9	23.5	20.6	12.5
SU-11	15.9	0.503	31.5	32.0	32.3	-0.9
SD-12	47.1	0.832	30.9	40.0	47.4	-18.5
SU-13	14.8	0.466	9.2	23.0	23.1	-0.4
SD-14	24.3	0.675	9.0	20.0	22.5	-12.5
SU-15	15.6	0.493	18.7	27.0	27.2	-0.7
SD-16	34.7	0.772	18.7	28.5	31.4	-10.1
SU-17	15.7	0.497	14.4	24.0	24.6	-2.5
SD-18	30.1	0.738	14.0	24.0	26.8	-11.7
SU-19	16.7	0.527	8.4	20.0	19.6	2.0
SD-20	25.1	0.685	7.5	20.7	21.8	-5.3
SU-21	17.1	0.538	3.7	22.0	19.4	7.3
SD-22	20.8	0.620	3.7	18.5	19.6	-5.9
SU-23	20.9	0.621	29.0	37.0	25.5	31.1
SD-24	50.5	0.843	30.2	41.5	51.5	-24.1
SU-25	20.5	0.615	8.2	19.0	20.1	-5.8
SD-26	28.7	0.725	8.2	24.0	25.1	-4.6
SU-27	18.7	0.577	16.6	25.0	24.2	3.2
SD-28	35.4	0.777	15.4	36.2	35.1	3.4
SD-30	56.0	0.859	34.1	56.0	60.5	-7.1
SU-31	25.6	0.691	6.6	20.5	22.7	-10.7
SD-32	32.2	0.755	6.7	27.0	28.4	-5.2
SU-33	23.1	0.658	6.1	18.7	20.6	-10.2
SD-34	29.2	0.730	6.4	22.5	24.9	-10.6
SU-35	21.5	0.632	5.9	19.8	18.0	9.1
SD-36	27.4	0.712	6.1	21.0	23.5	-11.9
SU-37	21.2	0.627	6.2	18.5	19.7	-6.5

*SU signifies a step-up of input velocity; SD signifies a step-down.

Table 3. (cont.)

Exp. No.	h_{ss}(cm.)	ϵ_{ss}	A(cm.)	T(sec.) exp.	T(sec.) cal.	%Δ
SU-38	20.0	0.605	9.6	20.5	19.4	5.4
SU-39	17.3	0.543	9.9	21.0	20.3	3.3
SU-40	22.8	0.654	6.5	24.5	21.3	13.1
SU-42	23.4	0.662	12.3	27.5	30.5	-9.1
SU-43	24.1	0.668	11.9	25.5	24.2	5.1
SU-44	18.1	0.563	9.6	24.5	25.6	-4.5
SU-45	17.5	0.549	6.5	22.5	24.4	-8.5
SU-46	17.5	0.549	6.5	23.5	24.4	-3.8
SU-47	29.1	0.729	9.6	31.1	28.8	7.4
SU-48	29.1	0.720	9.4	28.0	28.8	-2.9
SET III - 40 - 45 mesh particles, Bed wt. 400 gms. ρ_s 2.5 g./cc.						
SU-49	19.1	0.587	4.5	8.5	10.2	-20.0
SD-50	23.6	0.666	4.0	13.6	12.3	9.5
SU-51	19.1	0.586	5.1	8.6	9.1	-17.4
SD-52	24.2	0.673	4.9	11.8	11.7	0.8
SU-53	18.4	0.571	17.0	11.0	10.5	4.5
SD-54	35.4	0.777	16.9	19.4	18.5	4.6
SU-55	19.2	0.586	20.6	14.0	10.7	23.5
SD-56	39.8	0.801	20.5	19.5	21.8	-6.7
SU-57	26.2	0.698	3.9	11.5	13.0	-13.1
SD-58	30.1	0.738	3.6	11.5	15.1	-31.3
SU-59	25.3	0.687	5.4	10.8	12.6	-16.6
SD-60	30.6	0.742	5.7	12.9	15.2	-17.8
SU-61	23.8	0.667	8.2	10.5	12.1	-15.3
SD-62	32.0	0.752	8.3	13.9	16.1	-15.8
SU-63	21.3	0.628	7.2	10.3	10.8	-4.8
SD-64	28.4	0.722	7.1	13.3	13.7	-3.0
SU-65	21.1	0.625	14.3	11.2	10.7	4.5
SU-67	19.0	0.584	18.0	12.0	10.6	11.6
SD-68	36.1	0.780	17.6	15.0	18.3	-22.0
SU-69	16.5	0.520	7.2	6.5	7.3	-12.3
SU-71	15.6	0.493	10.1	10.0	10.8	-8.0
SU-73	26.0	0.685	6.7	13.5	13.2	2.2
SD-74	32.7	0.758	6.3	18.3	16.4	10.4
SU-75	16.1	0.509	23.8	12.4	10.6	14.5
SU-77	32.8	0.793	16.1	19.5	20.1	-3.1
SU-79	36.1	0.781	4.7	18.4	18.9	-2.7
SD-80	40.8	0.806	3.8	18.4	22.3	-21.2

Table 3. (cont.)

Exp. No.	h_{ss}(cm.)	ϵ_{ss}	A(cm.)	T(sec.) exp.	T(sec.) cal.	%Δ
SU-81	26.2	0.698	4.8	17.5	13.0	25.7
SU-82	18.3	0.567	7.7	10.2	9.8	3.9
SU-83	18.5	0.572	6.5	10.3	10.0	2.9
SU-84	22.6	0.650	11.6	12.5	11.7	6.4
SU-85	24.3	0.674	11.6	11.4	12.1	-6.1
SU-86	24.0	0.670	3.4	11.5	11.8	-2.6
SU-88	20.6	0.616	18.4	15.0	12.9	14.0
SU-89	20.7	0.618	21.3	14.5	13.1	9.6
SU-90	21.0	0.623	15.3	11.4	11.6	-1.8
SU-91	21.2	0.627	16.0	11.4	11.5	-0.9
SU-92	21.4	0.630	4.9	11.0	11.6	-5.5
SU-94	21.3	0.628	10.7	13.9	11.6	16.5
SU-95	22.7	0.652	11.8	14.5	12.0	17.2
SU-96	22.6	0.650	14.6	15.6	12.3	14.7
SU-97	23.3	0.660	17.1	14.8	13.3	10.1
SU-98	23.3	0.660	21.0	12.0	13.3	-10.8
SU-99	23.9	0.669	21.6	12.9	12.0	7.5
SU-100	24.0	0.670	15.0	16.0	12.3	23.0
SU-101	24.4	0.675	11.4	15.0	12.8	14.6
SU-102	24.2	0.673	16.4	15.2	12.3	19.1
SET IV - 25-30 mesh particles, Bed wt. 200 gms., ρ_s 1.08 g./cc.						
SU-103	27.2	0.660	25.4	60.0	67.1	-11.8
SU-104	23.1	0.599	24.1	41.0	48.7	-18.8
SU-105	20.4	0.547	26.1	57.0	59.9	-5.1
SU-106	20.2	0.543	11.6	46.5	53.2	-14.4
SU-107	22.5	0.590	12.3	46.5	51.2	-10.1
SU-108	23.8	0.612	18.8	49.5	51.9	-4.8
SU-109	19.9	0.535	11.1	44.0	48.4	-10.0
SU-110	19.6	0.528	16.0	49.0	48.2	1.6
SU-111	19.8	0.533	8.2	52.4	48.4	7.6
SD-112	26.6	0.652	6.6	63.7	58.6	8.0
SU-113	20.1	0.539	12.7	51.5	48.6	5.6
SD-114	32.8	0.718	12.5	68.7	71.5	-4.7
SU-115	23.3	0.603	17.7	50.5	51.2	-1.4
SD-116	41.3	0.776	17.3	71.0	78.8	-11.0
SU-117	25.3	0.635	10.9	44.0	55.9	-27.1
SD-118	36.2	0.744	7.2	56.3	74.6	-32.5

Table 4. Values of $t_{0.02}$ in seconds.

Exp. No.*	$t_{0.02}$	Exp. No.	$t_{0.02}$	Exp. No.	$t_{0.02}$
SU-2	50	SD-28	6	SD-68	2
SU-3	46	SD-30	9	SU-71	10
SU-4	55	SU-31	27	SU-73	4
SD-5	12	SD-34	5	SD-74	6
SD-6	7	SU-35	34	SU-75	28
SU-7	75	SD-36	7	SU-77	30
SU-8	17	SU-49	4	SU-79	6
SU-9	18	SU-50	6	SD-80	3
SU-11	88	SU-51	20	SU-82	6
SD-12	8	SD-52	7	SU-85	23
SU-13	45	SU-53	36	SU-89	19
SD-14	13	SD-54	6	SU-106	35
SU-15	80	SU-55	37	SU-107	33
SD-16	7	SD-56	2	SD-112	13
SU-17		SU-57	4	SU-113	26
SD-18	8	SD-58	3	SD-114	18
SU-19	35	SU-59	3	SU-115	85
SD-20	13	SD-60	4	SD-116	16
SU-21	38	SU-61	5	SU-117	70
SD-22	12	SD-62	3	SD-118	11
SU-23	150	SU-63	12		
SD-24	13	SD-64	2		
SU-25	44	SU-65	17		
SD-26	7	SU-67	27		

*SU signifies a step-up of input velocity; SD signifies a step-down.

Response to Pulse Input

A considerable amount of pulse data was taken in the manner described in the experimental section. Figure 10 shows the response observed for a representative experimental run. A discussion of the deviation of the experimental response from the model can be found in the section, "Deviations from the Model." The purpose for obtaining data in this form was to convert it to frequency response data by an approximate Fourier transform technique. Hougen and Walsh (6) have discussed "pulse testing" as a convenient method of obtaining frequency response data. A pulse is described as a function which differs from zero for a finite time only. The form of the pulse applicable to the pulse testing method is arbitrary and in these experiments consisted of a combination of two step changes as previously described.

A time function, f(t), is composed of an infinite number of harmonic components. The resolution of these components is accomplished by evaluation of the Fourier transform

$$F(i\omega) = \int_0^\infty f(t)\, e^{-i\omega t}\, dt \qquad (35)$$

A method and tables for evaluation of this integral are given by Huss and Donegan (7). The method presented consisted of representing f(t) by a staircase function consisting of n equal intervals. This procedure is shown in Figure 11. The Fourier transform in terms of the transfer function becomes

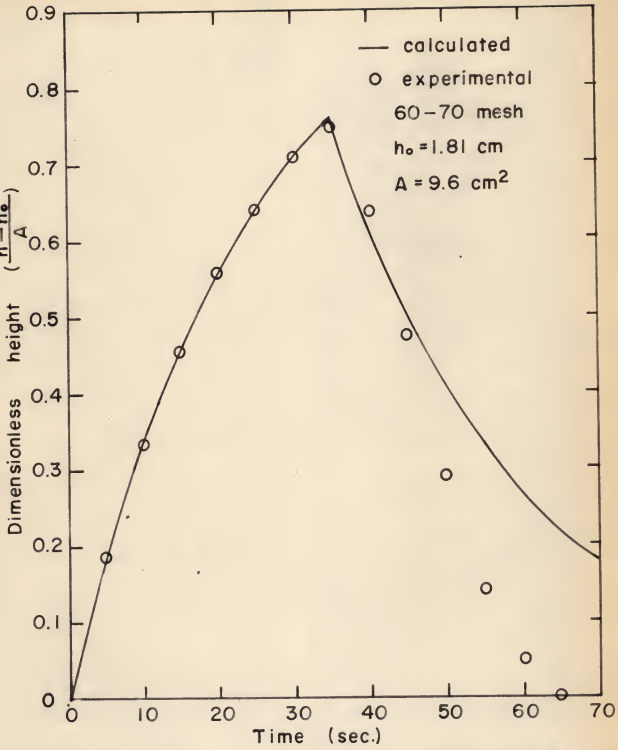

Fig. 10. Response of liquid-solid fluidized bed to pulse input.

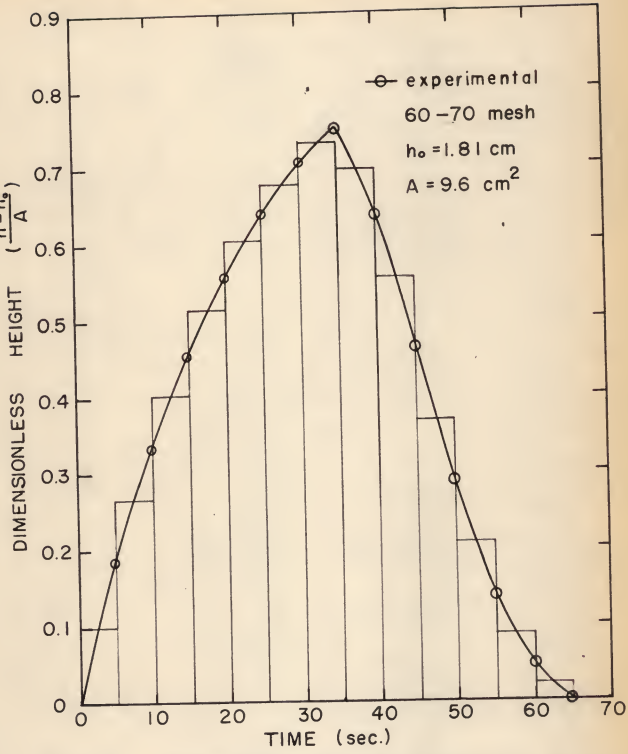

Fig. 11. Approximation of response to pulse input by Staircase function.

$$F(i\omega) = \sum_{n=1}^{\infty} F_n(i\omega) \tag{36}$$

where

$$F(i\omega) = \int_{t_{n-1}}^{t_n} r_n e^{-i\omega t}\, dt \tag{37}$$

The real part of Equation (37) is

$$R_n\left[F(i\omega)\right] = r_n \frac{2}{\omega} \sin\left(\frac{\Delta t}{2}\omega\right) \cos\left[(2n-1)\frac{\Delta t}{2}\omega\right] \tag{38}$$

and the imaginary part is

$$I_n\left[F(i\omega)\right] = r_n \frac{2}{\omega} \sin\left(\frac{\Delta t}{2}\omega\right) \sin\left[(2n-1)\frac{\Delta t}{2}\omega\right] \tag{39}$$

where r_n is the height of the staircase function and Δt is the time interval.

The real part of the total Fourier transform of the function is the sum of the real parts of the individual intervals.

$$R\left[F(i\omega)\right] = \sum R_n\left[F(i\omega)\right] \tag{40}$$

and the imaginary part is the sum of the imaginary parts of the intervals

$$I\left[F(i\omega)\right] = \sum I_n\left[F(i\omega)\right] \tag{41}$$

Letting $z = \frac{\Delta t}{2}\omega$ in Equation (38), Equation (40) becomes

$$R\left[F(i\omega)\right] = \Delta t \sum r_n \frac{\sin z \cos(2n-1)z}{z} \tag{42}$$

and from Equation (39) and Equation (41)

$$I\left[F(i\omega)\right] = -\Delta t \sum r_n \frac{\sin z \sin(2n-1)z}{z} \qquad (43)$$

The modulus of the Fourier transform is

$$A(\omega) = \sqrt{\left\{R\left[F(i\omega)\right]\right\}^2 + \left\{I\left[F(i\omega)\right]\right\}^2} \qquad (44)$$

and the phase angle

$$\theta(\omega) = -\tan^{-1}\frac{I\,F(i\omega)}{R\,F(i\omega)} \qquad (45)$$

The evaluation of Equations (42) and (43) is simplified by use of tables in which values of the functions $\frac{\sin z \cos(2n-1)z}{z}$ and $\frac{\sin z \sin(2n-1)z}{z}$ are tabulated for values of n and z (7). The amplitude ratio can be determined as

$$A.R. = \frac{A(\omega)_{output}}{A(\omega)_{input}} \qquad (46)$$

and the phase lag is

$$\alpha = \theta_{input} - \theta_{output} \qquad (47)$$

This calculation was carried out for experimental pulse inputs of from 15 to 30 second duration. One of the better response curves obtained is presented in Figure 12.

The pulse testing technique requires that the system be linear. Application to a non-linear system will not give meaningful results unless the disturbance considered is small enough for

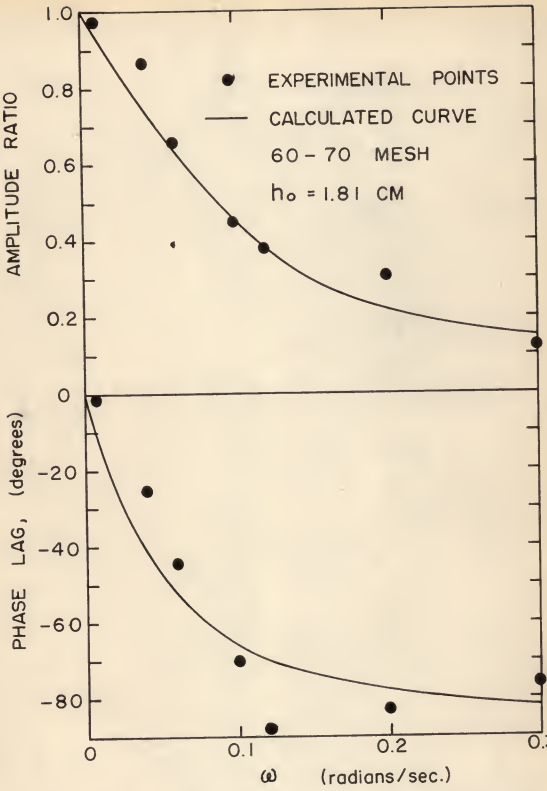

Fig.12. Frequency response of liquid-solid fluidized bed from pulse input.

the system to behave linearly. When the pulse data were being taken it was not known whether this condition was being fulfilled or not. However, due to the rather odd shape of the response curve, particularly that for phase lag, it was considered necessary to measure the actual response to a sinusoidal input.

Response to Sinusoidal Input

Two types of data were taken on the response to a sinusoidal input. The first was bed height versus time data. This was done in order to determine the degree of distortion in the output. A linear system will produce a response to a sinusoidal input which is also sinusoidal. Non-linearities will, however, tend to cause deviations from the sine wave form. No attempt was made to quantitatively analyze the distortion, but a graph illustrating this behavior is presented in Figure 13.

The second type of data taken was used in the determination of amplitude ratio and phase lag relationships. Amplitude ratio is defined by

$$A.R. = \frac{\text{amplitude of output}}{\text{amplitude of input}} \tag{48}$$

The output amplitude was determined as the difference between the maximum and minimum in bed height expansion divided by two. The input amplitude was a sinusoidally varying flow rate. For use in computation, this had to be converted into the same units as the output amplitude. This was accomplished by use of the steady-state curve relating bed height and flow rate for the system

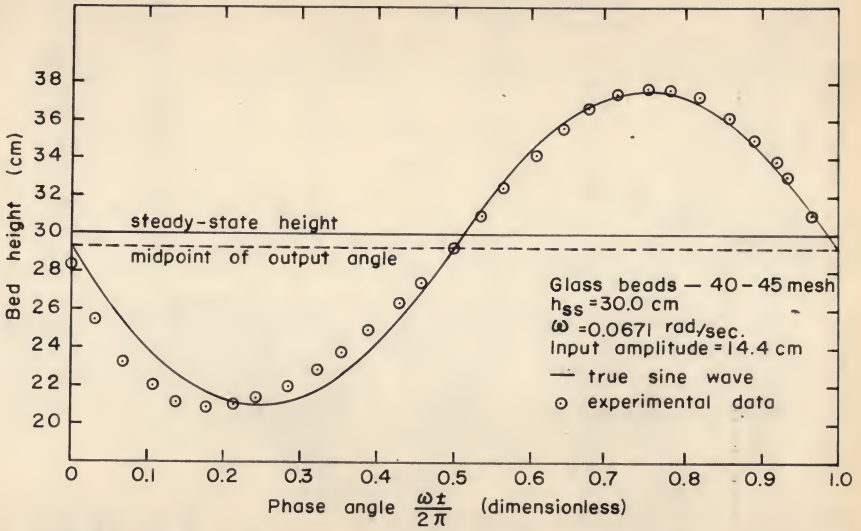

Fig. 13. Bed height vs. phase angle for sinusoidal input in fluidizing velocity.

being studied. The procedure used is illustrated in Figure 14. In this figure, the input flow amplitude is 0.32 cm./sec. and the steady-state flow, 2.16 cm./sec. Thus, the maximum and minimum in flow are 2.48 cm./sec. and 1.84 cm./sec. respectively. The steady-state heights corresponding to these flows are 37.0 cm. and 25.0 cm. This gives an amplitude in terms of bed height expansion of $\frac{37.0-25.0}{2}$ 6.0 cm. The mechanism by which the mechanical sine wave generator produces a given amplitude in flow can be seen by referring to Figure 5. From the expression

$$V = A_{cy} V_L \sin\beta \tag{49}$$

it is obvious that the flow, V, is a maximum when $\beta = \pi/2$ and a minimum when $\beta = 3\pi/2$. The values of these extremes are

$$V^* = \pm A_{cy} V_L \tag{50}$$

The tangential velocity, V_L, is given by

$$V_L = L\omega \tag{51}$$

where L is the length of the lever arm and ω is the frequency. Therefore, from Equation (50)

$$V^* = \pm A_{cy} L\omega \tag{52}$$

or in terms of superficial velocity

$$\frac{V^*}{A_{col}} = \phi^* = \frac{A_{cy}}{A_{col}} L\omega \tag{53}$$

where ϕ^* is the superficial liquid velocity amplitude and A_{col} is

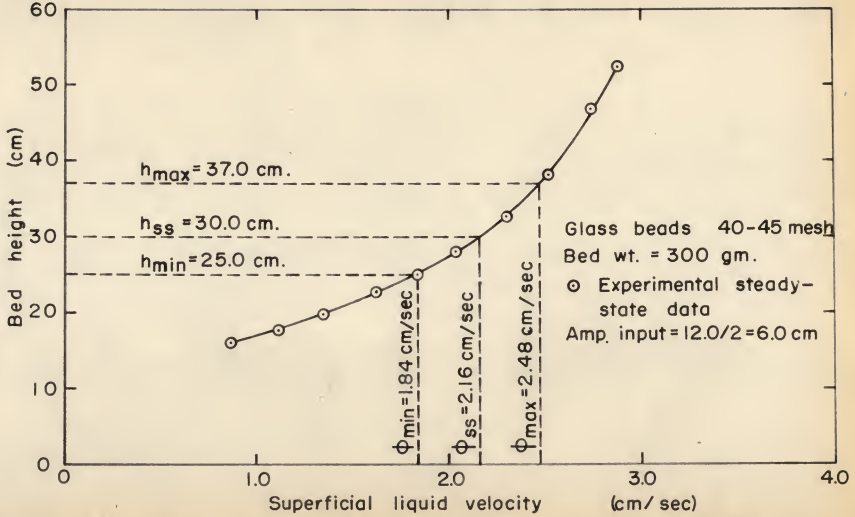

Fig. 14. Determination of experimental input amplitude for sinusoidal input.

the cross-sectional area of the column. Thus various input amplitudes were obtained by varying the values of L and ω.

The experimental phase lag was determined by obtaining the time interval between the reversal in piston motion and the reversal in bed height motion. The phase lag was then determined as

$$\tan (90^\circ - \varphi) = \frac{4\omega(\Delta t)}{2\pi} \qquad 0^\circ \leq \varphi \leq 90^\circ \qquad (54)$$

where φ is the phase lag and Δt is the time interval between reversal in the direction of piston motion and the reversal of bed height motion. This method was very limited since Δt is quite small at high frequencies and could not be measured by observation. Another limitation lies in the fact that the wave form of the output is distorted as illustrated in Figure 13.

Amplitude and phase lag data are shown plotted against frequency in Figure 15 for the 6 to 7 mesh glass particles. In this series of experiments no attempt was made to hold the input amplitude constant for each experiment. The input amplitude range is from 4.05 cm./sec. to 0.494 cm./sec. or from 10.4 cm. to 1.4 cm. in terms of bed height expansion. These data are shown compared with the response calculated by the linearized model.

DISCUSSION OF RESULTS

At this point it would be desirable to emphasize the purpose of the work. The basic desire was to develop a linearized model to describe the dynamic behavior of liquid-solid fluidized beds and to show by experiment that the model is sufficiently accurate

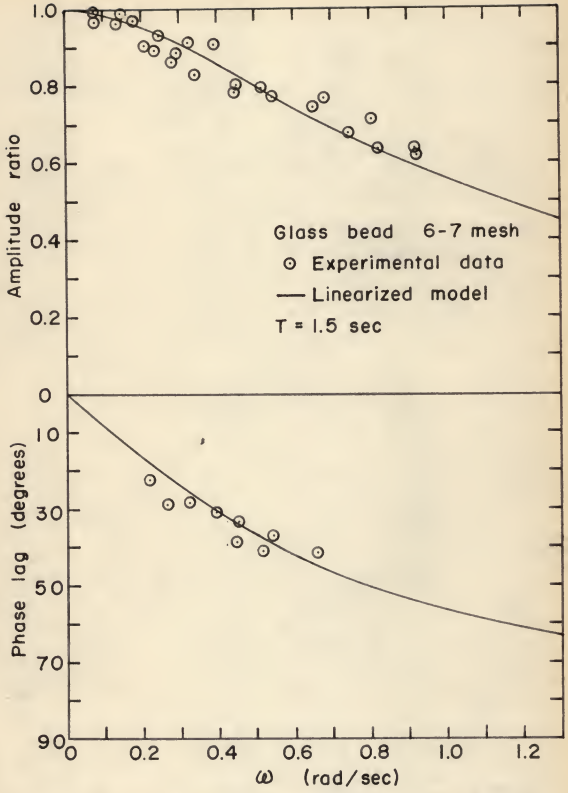

Fig. 15. Frequency response of liquid–solid fluidized bed for 6–7 mesh glass beads.

for control purposes. Many non-linear flow processes are treated in this manner for the purpose of analyzing and synthesizing process control systems. Any fluid flow or heat transfer process will exhibit non-linearities due to the dependence of transport properties on the values of such intensive variables as temperature and pressure. For example in heat transfer the conductivity of a material is dependent on the temperature, and in fluid flow the resistance to flow is usually dependent on Reynolds number, which is a function of fluid density, velocity, and viscosity. In some instances it is possible to very nearly approximate system behavior by a linear differential equation; while in other cases this might not be true. The accuracy with which a system may be approximated is usually dependent on the relationship between the steady-state behavior of the system and the independent variables. If this relationship were linear, we could employ a linear differential equation to describe the dynamic behavior of the system exactly. Therefore, we should examine the steady-state relationship between fluidizing velocity and porosity or bed height. This relationship is given by Richardson, et. al. (4) as

$$\phi_{ss} = U_g \epsilon_{ss}^{n}.$$

Since porosity is the independent variable in this case it would be well to rewrite this relationship as

$$\epsilon_{ss} = k \phi_{ss}^{1/n}$$

where

$$k = 1/U_s^{1/n}.$$

The terminal falling velocity, U_s, will remain constant when the fluid viscosity and density are constant. Therefore, non-linearity of this curve depends on the value of 1/n. From Equations (28) to (31) it is seen that in the usual range of operation, the value of n ranges from 2.59 to 4.65. Values of n within this range do not depart sufficiently from one to make linearization impractical.

There is, however, another factor which makes fluidization very difficult to analyze from a dynamic standpoint. This involves the mechanism of bed expansion and contraction. As shown by Slis, et. al., (5), the mechanism for expansion is different from that for contraction. Because of this difference between expansion and contraction, the response to a decreasing flow rate differs from that to an increasing flow rate. Therefore it is impossible to describe the dynamic behavior of a fluidized bed accurately by one model. This is true whether the model is linear or non-linear. It should, however, be possible to describe the dynamic behavior for small fluctuations by a single, linear, model and this is what has been attempted. The necessity for this type of representation is obvious when it is considered that the deviations which might occur in an actual process are random.

Effect of Changes in Temperature on the Time Constant, T

Since many processes may be subject to changes in fluid temperature it is necessary to consider such effects on the time constant of the process. The expression for the time constant, T,

is given as

$$T = \frac{h_{ss}}{nU_s \epsilon_{ss}^{n-1} (1-\epsilon_{ss})}$$

or the equivalent expression

$$T = \frac{h_{ss} \epsilon_{ss}}{n \phi_{ss} (1- \epsilon_{ss})}$$

At a constant bed height and porosity the dependence of T on temperature is seen to involve the changes of n and ϕ or n and U_s. Since n is an empirical function of Reynolds number and U_s is a function of liquid density and viscosity it would be useless to try to develope an analytical expression for this effect. In Table 5, however, values of T are given as a function of temperature for a system consisting of water and 40 to 45 mesh glass beads. Table 5 shows that a considerable change in time constant, T, might be expected when temperature variations of $\pm$ 50°F or greater are encountered. For smaller changes in temperature this effect would probably not be important.

Deviations from the Model

For the response to a step input, there are two types of deviations to be considered. The first involves the deviations of the time constants calculated by the linearized model from the experimental time constants. These deviations, expressed in percentage, have been tabulated for each experimental run in Table 3. By considering both positive and negative deviations, the average

Table 5. Dependence of T on Temperature.

Particles: 40 - 45 mesh glass beads (ρ_p 2.5 g./cc.)

Fluid: Water, h_{ss} = 25 cm. ϵ_{ss} = 0.600.

Temp. (°F)	U_s (cm./sec.)	n	T (sec.)
50	4.00	3.46	15.86
75	4.45	3.33	13.83
100	4.98	3.21	12.05
150	6.24	3.00	9.28
200	7.53	2.82	7.48

deviation for all experimental runs was -2.1 %. Since no systematic variation in these deviations could be related to any of the operational variables such as bed height, porosity, or size of step, it must be assumed that they are the result of inaccuracies in calculation and the inherent inaccuracy in the graphical method of obtaining experimental time constants. On the other hand, the time interval over which the experimental response follows the linearized model is definitely a function of the operating conditions. This has been shown in a previous section where $t_{0.02}$ was tabulated for each run. It is evident that in general the response to a step up is described accurately over a much greater time interval than the response to a step down. Because of this it is necessary to consider the response to a step down in flow in order to determine the limitations on the applicability of the linear model.

Slis, et. al. (5) have shown that the response to a step down in flow can be considered a special case of sedimentation. Therefore, we expect a constant bed height velocity resulting in a straight line response of bed height to a step-down in fluidizing velocity. This response can be represented by

$$h = (\phi_1 - \phi_{ss})\, t + h_{ss} \tag{55}$$

where ϕ_1 is the superficial liquid velocity after the step input. The linearized model, however, gives a response of

$$h = A\,(1-e^{-t/T}) + h_{ss} \tag{56}$$

rearranging (55) and (56) and taking their difference gives

$$\left(\frac{h-h_{ss}}{A}\right)_{hyp} - \left(\frac{h-h_{ss}}{A}\right)_{cal} = kt - (1-e^{-t/T}) \qquad (57)$$

where $k = \left(\frac{\phi_1 - \phi_{ss}}{A}\right)$. Here the subscript (hyp) stands for a hypothetical response based on Equation (55) and (cal) for the response calculated from the linearized model. Comparing Equation (57) with Equation (34) it is seen that

$$k\, t_{0.02} - (1-e^{-\frac{t_{0.02}}{T}}) = 0.02 \qquad (58)$$

This can be rewritten as

$$e^{-\frac{t_{0.02}}{T}} + k\, t_{0.02} = 1.02 \qquad (59)$$

Equation (59) can be further simplified by noting that $\Delta\phi = \frac{A}{T}$ from Equation (13). Since $k = \frac{\Delta\phi}{A}$, we can write

$$k = \frac{A/T}{A} = \frac{1}{T} \qquad (60)$$

and (59) becomes

$$e^{-\frac{t_{0.02}}{T}} - \frac{t_{0.02}}{T} = 1.02 \qquad (61)$$

Now Equation (61) is a single valued function of $(t_{0.02})$ so that there will be only one value of $(\frac{t_{0.02}}{T})$ which will satisfy it. This is graphically found to be $(t_{0.02}/T) = 0.205$. The actual

values of $\frac{t_{0.02}}{T}$ from Tables 3 and 4 vary from 0.1 to 0.35 with a mean of 0.22. Part of this error is undoubtedly due to the trial and error method of obtaining the $t_{0.02}$ and the remainder to the inaccuracy of Equation (61). Equation (61) would, however, be an acceptable means of estimating the deviation to be expected when applying the linearized model to a step-down in fluidizing velocity. It should be emphasized that the value 0.02 was chosen arbitrarily and that any desired value may be picked. This is shown by writing Equation (61) in the more general form

$$e^{-t/T} + \frac{t}{T} = f\ (t/T) \tag{62}$$

where

$$f(t/T) = 1 + \left(\frac{h-h_{ss}}{A}\right)_{hyp} - \left(\frac{h-h_{ss}}{A}\right)_{cal} \tag{63}$$

Therefore any desired value of $\left(\frac{h-h_{ss}}{A}\right)_{hyp} - \left(\frac{h-h_{ss}}{A}\right)_{cal}$ can be chosen and the corresponding value of (t/T) calculated. To facilitate this determination, a plot of f(t/T) versus t/T is given in Figure 16.

The response to a step-up in fluidizing velocity is generally approximated very closely by the linear model over a long time interval. An interesting phenomenon which was observed concerning the response to a step-up was the development of an irregularity in the response curve when the input was quite large. It is not known whether this was due to some experimental error or whether it is inherent in the response to a step-up in fluidizing velocity. The development of this irregularity is shown in Figures 17a, 17b

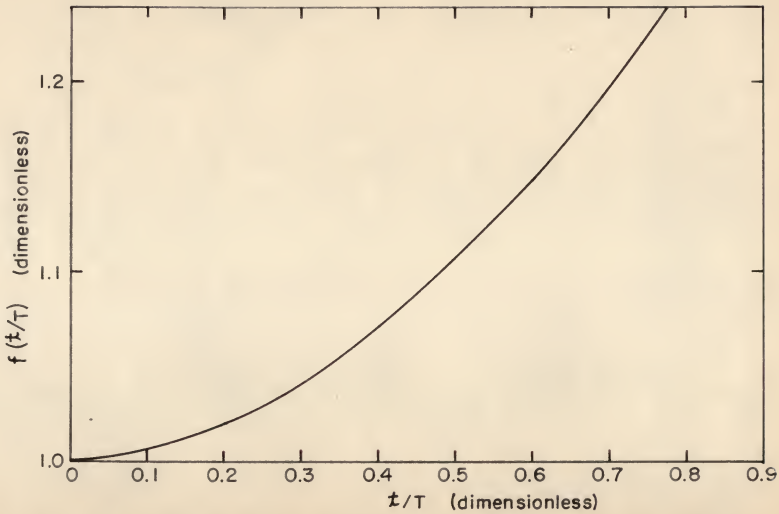

Fig. 16. Graph for determining limitation of linear model to represent response to step change.

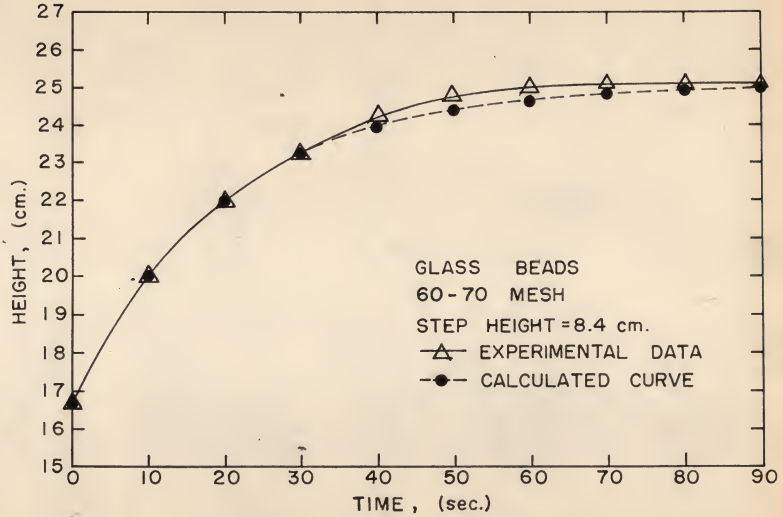

Fig. 17-A. Time vs. height for step input.

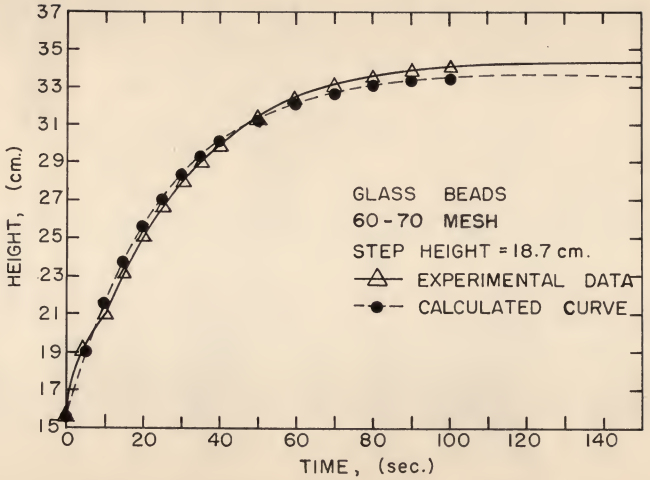

Fig.17-B. Time vs. height for step input.

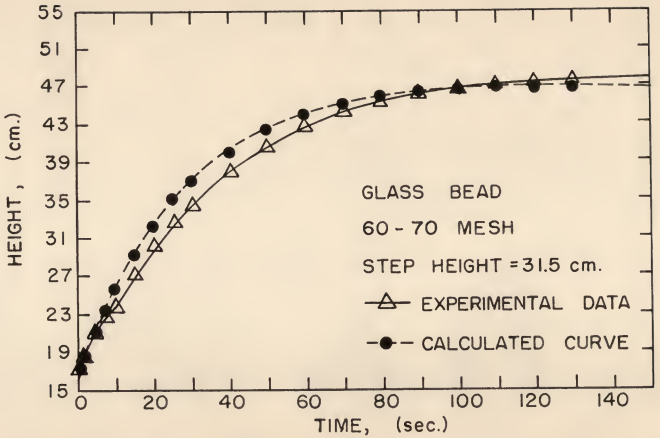

Fig. 17-C. Time vs. height for step input.

and 17c. As can be seen, the linearized model will adequately represent the response over this irregularity, but deviates thereafter. Although this behavior is interesting, it probably would not ordinarily be of practical interest since the irregularity was never observed to develop except when the disturbance was of a magnitude equivalent to the steady-state height. In process control applications it is improbable that disturbances of this magnitude would be encountered.

The same non-linearities which caused deviations in the response to a step input were also found significant in the frequency response analysis.

Insufficient frequency response data has been obtained to permit a complete analysis of the deviations of this response from the model and about all that is possible is a qualitative description. Figure 13 showed that a small amount of distortion in the output wave form was obtained. This is reasonable and can be attributed chiefly to two sources. First, the input in terms of flow rate is a true sine wave (subject to experimental error), but the input in terms of equivalent bed height is not. This is because of the non-linear nature of the steady-state relation between bed height and fluidizing velocity which has been clearly illustrated in Figure 14. Therefore, since the input is not exactly sinusoidal, we could not expect the output to be. This source of distortion is, of course, dependent on the input amplitude and becomes negligible as the input amplitude approaches zero. The second source of output distortion is the difference in the mechanisms for expansion and contraction of the bed. This

effect could be quite important and should not be particularly related to the input amplitude. Therefore a small amount of distortion can be expected for any input amplitude. It should be noted that the response curve presented in Figure 13 is the result of rather extreme conditions. The input amplitude in this case is 14.4 cm. or approximately 0.5 h_{ss}. Also, the manner of constructing Figure 13 tends to concentrate all of the distortion in the lower half of the curve. The reason for this is that one experimental point had to be selected as a reference point for the remainder of the curve. This was chosen as the point at $(\frac{\omega t}{2\pi})$ equal to 0.75. In the actual response it is doubtful that all of the distortion would be concentrated in one area of the curve as it is shown. The author feels, however, that due to the mechanism for bed contraction, (the bed tends to contract at a higher rate than it expands for the same input), more distortion would be expected in the lower half of the cycle than in the upper half and Figure 13 was constructed in such a manner to emphasize this.

Very little data was obtained on the phase lag relationship. Experimental limitations of the procedure as described and the distortion in the output wave made this data very difficult to obtain and interpret. The limited amount of data presented was obtained by averaging the phase lag at the top of the cycle with that at the bottom. This procedure generally gave results in fairly good agreement with the linearized model. One point in question at this time concerns the limits of the phase lag when expressed as a function of frequency. The first order linear model predicts that the lag should be zero degrees at a frequency of zero and

approach 90 degrees as the frequency approaches infinity. This behavior was borne out over the entire experimental range except at the maximum frequency obtainable with the equipment. At this frequency, approximately 0.92 rad./sec., it appeared that the phase lag was just over 90 degrees. This behavior did not manifest itself to a sufficient degree at this frequency that any definite conclusions could be drawn and it was impossible to obtain higher frequencys with the equipment as constructed. This would be an interesting area for investigation, however, since greater lags than 90° would suggest the propriety of models of higher order than one.

The amplitude ratio-frequency relationship is probably the most significant tool which the field of process dynamics has to offer for use in the design and evaluation of processes. It was found that the first order linear model could be used to represent this relationship quite accurately for reasonable input amplitudes ($\Delta h < 0.5\ h_{ss}$). It is not known exactly to what degree of accuracy the model could be expected to approximate any given system, but it seems likely that it could be depended on to yield results satisfactory for preliminary design calculations. In addition to the results given in Figure 15 for 6 to 7 mesh glass beads with a variable input amplitude, additional amplitude ratio data are presented in Figure 18. The agreement of the data shown with the curve calculated using Equation (23) is very good.

A final point on the deviations encountered in the response to a sinusoidal input is concerned with the "shift" in the steady-state height, h_{ss}, which was observed. This can be seen in Figure

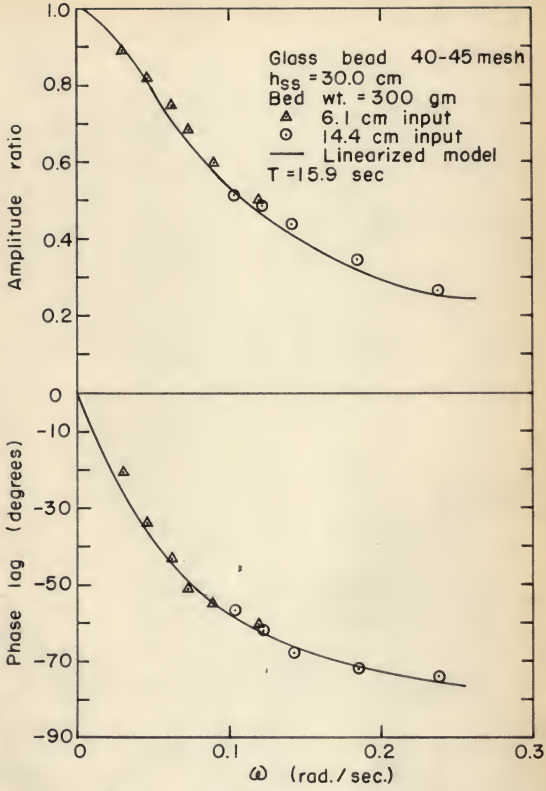

Fig. 18. Frequency response of liquid-solid fluidized bed for 40-45 mesh glass beads.

13. There, the midpoint of the output cycle falls about 0.7 cm. below the steady-state height. This behavior was observed in all of the experiments and the "shifts" were usually downward. From Figure 14 it would seem that any change in h_{ss} should be upward and in some cases a slight tendency toward this was observed. In all other cases it seems that some other factors outweigh the effect shown in Figure 14. This was probably caused by the tendency for the bed to contract more rapidly than to expand as mentioned previously.

Application of Pulse Testing Method to Fluidization

As has been indicated, an attempt was made to obtain frequency response data from the response to a pulse input. An example of the results obtained was presented in Figure 11. The results were generally very erratic and in many cases the amplitude ratio would not approach one as the frequency approached zero. Also there was a tendency for the analysis to yield very high values at a frequency around 0.4 rad./sec. At intermediate frequencies, (0.1 - 0.3 rad./sec.), the method usually gave reasonable results. The poor results at high and low frequencies could be caused partly by a deficiency in the harmonic content of the pulse. The pulse used was a rectangular one and the response to this pulse form is very limited in harmonic content. It would be advisable to employ a more irregular pulse input in any further work along this line. The non-linearity of the system also contributes very definitely to the erratic results. It must be concluded that pulse

testing is not an advisable manner in which to obtain frequency response data for bed height change in fluidization processes.

Comparison of Results with Those of Other Investigations

There are only two references to the authors knowledge which present any results on the study of transient behavior of the fluidized bed. The first of these is a paper by Slis, et. al. (5) in which the response to a step input in fluidizing velocity is considered. The data given in that paper is not of such a nature that a direct comparison can be made with the results of this present work. The experimental responses observed were similar with a single exception which will be discussed under the topic of "Effect of Particle Size Distributions."

The second reference is a technical report by Martin Nuclear Company (8). In this report the following differential equation was derived to represent the transient behavior of fluidized bed height.

$$\frac{d^2L}{dt^2} = \frac{g(\rho_p - \rho_c)}{\rho_p} \quad \frac{d^3u_o}{\epsilon}\, 3b\text{-}2 \left(\frac{u_o}{\epsilon} - \frac{dL}{dt}\right)^2 - 1 \qquad (63)$$

where L is the bed height, ρ_p the solid density, ρ_c the liquid density, g the gravitational constant, u_o the superficial liquid velocity, ϵ the porosity, and b is a constant defined by the equation $\epsilon_{ss} = du^b_{o_{ss}}$.

No experimental data was presented, but Equation (63) was programed on an analog computer and the traces for various inputs reproduced. The linear, first order model was used to calculate the response to these same inputs and the results are given in Figure 19. A detailed description of the manner in which the calculations were made to obtain the response given by the linearized model is presented in Appendix B. Figure 19 represents only a comparison between the two models since no experimental data is available with which to compare the response given by Equation (63). The curve labeled "Response by Equation (63)" is an analog response which was given in reference (8). This represents an interesting application of the linearized model, however, since the operating conditions differ widely from those of the experimental conditions existing in this present work. This can be seen by referring to Appendix B.

Effect of Particle Size Distributions

This discussion was prompted by a discrepancy in the experimental results of this work and the results presented in a paper by Slis, et. al. (5). They reported an experimental response to a step-up in flow which was linear for the first part of the response. It turned out, in fact, that the time interval over which this linear response was observed was defined by

$$0 < t < t^*$$

where

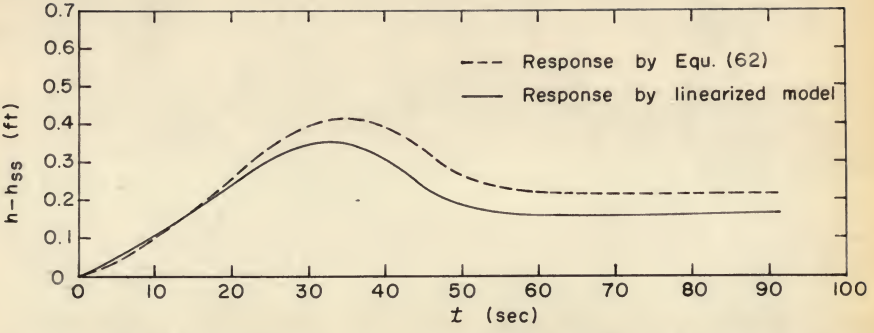

Fig. 19. Comparison of linearized model with Equation (62).

$$t^* = \frac{\epsilon_{ss} h_{ss}}{n \phi_{ss} (1 - \epsilon_{ss})} \tag{64}$$

It should be noted that this equation for t* is the same equation used to calculate T. In this present experimental work the time constant, T, was usually in the neighborhood of 10-20 seconds. It should have been possible to detect this linear relationship quite easily, but it was not observed. The response to a step-down was quite definitely linear as predicted in reference (5). This agreement in one case and disagreement in another related case is very perplexing. A possible explanation involves the effect of particle size distributions on the response of fluidized beds to upsets. In any fluidization process there will be a certain range of particle diameters. If all of the particles are of uniform density, as is usually the case, the smaller particles will tend to concentrate at the top of the bed and the larger particles at the bottom. Therefore we might expect a somewhat continuous axial distribution of particle sizes. For particles of uniform density, the terminal falling velocity will increase with increasing diameter. This will also cause an increase in Reynolds number and a corresponding decrease in the empirical constant, n. However, the increase in U_s will always be proportionally greater than the decrease in n. Referring to Equation (17) it is seen that the time constant will decrease with increasing particle diameter due to the effects described above and larger particles can be expected to show a faster response to upsets than smaller particles. Now if the bed is at a steady-state condition and is

subjected to a step-up in fluidizing velocity, the particles at the top of the bed, the smaller particles, will respond slowly with an increase in response speed as we go toward the bottom of the bed. The initial response of bed height will be due almost entirely to these slowly responding particles at the top of the bed, but there will be considerable particle mixing and interaction within the bed and as a result the particle distribution at the top of the bed will be continually changing and yielding different response characteristics. It must be pointed out that this discussion pertains to the condition at the top of the bed at times before t*. After t* which denotes the time at which a disturbance is to reach the top of the bed there will definitely be a change in porosity at this point and this will cause varying response characteristics. When considering the response to a step-down the situation is reversed. The particles at the bottom will still respond faster, but the deviation of this response is away from the top of the bed. The particles within the bed will not be affected greatly by particles below them and the entire bed will settle much as in sedimentation.

The smaller the particle size range, the more neglible the effects described above would be. It is supposed that the particles used by Slis et. al. (5) were very uniform. It is important to be conscious of the phenomena described, however, since in most applications, there is a sizeable particle size range.

Effect of Aggregative Fluidization

It was previously mentioned that this work was to deal chiefly with particulate fluidization. This was specified since the task of analyzing the unsteady state of fluidization processes would be greatly magnified if non-idealities were present in the steady-state condition other than the essential non-linear characteristics. It is however deemed advisable to at least mention the area of aggregate fluidization since most of the fluidization processes fall into this category. This is particularly true of gas-solid fluidization and several sources have recently reported having observed it in liquid-solid systems (9). In liquid-solid fluidization aggregative fluidization occurs when large, heavy particles are fluidized with a relatively non-viscous liquid such as water.

In this present investigation a tendency toward aggregate fluidization was observed when fluidizing the 6 to 7 mesh glass beads. Two distinct phases were observed. One consisted of areas densely populated with particles and the other of "bubbles" of water traveling up through the bed. Frequency response experiments were carried out on this system and the data obtained were quite satisfactory. A problem was encountered in trying to apply the linearized model to this case, however. The terminal falling velocity of the particles was determined and n calculated by the appropriate correlation. These values were 35.8 cm./sec. and 2.39 respectively. For particulate fluidization, therefore, one would expect a steady-state relationship from Richardson and Zaki (4) of the form

$$\phi_{ss} = U_s \in_{ss}^{n} = 35.8 \in_{ss}^{2.39}$$

For aggregate fluidization this is no longer valid. From steady-state data obtained for this system it was found experimentally that the relationship

$$\phi_{ss} = a \in_{ss}^{b} \tag{65}$$

could be used to represent the data. For this case a was found to be 23.8 and b was determined as 2.5. It was found that use of the values of U_s and n in determining the system time constant gave satisfactory results even though these are not the same as the experimental parameters for the steady-state relationship. This value of T was 1.5 sec. It can be seen from Figure (15) that use of this time constant gave good agreement with the experimental data. This indicates that for liquid-solid aggregative fluidized beds, the dilute phase does not contribute significantly to the time constant of the system. Although there is no theoretical development to support this procedure, it is proposed as a possible method of determining the transient behavior of aggregative fluidized beds.

Application of the Linearized Model to Other Systems

The question which naturally arises at this point is whether or not the theoretical model can be applied to systems other than those on which experimental data were obtained. This is obviously very difficult to predict for an investigation of this nature.

However, if it is realized that the treatment presented is an approximation based on verified steady-state relationships, it would seem that the model could be expected to represent the response for any system to small disturbances where reliable steady-state data is available. It is possible that the model could be used to represent gas-solid systems as well as liquid-solid systems if the procedure outlined in the section on aggregate fluidization is followed. However, much more experimental work is needed before the general applicability of the model is proved.

CONCLUSIONS

The following conclusions have been drawn as a result of this investigation.

1. Fluidization processes are extremely difficult to analyze from a dynamic standpoint. This is due first to the nonlinear relationship between bed porosity and fluidizing velocity and second to the different mechanisms for bed expansion and bed contraction. It would not be possible to develop a single model to represent accurately all transient effects of a fluidized bed.
2. The results of this work should prove useful in process control. It has been shown that the response of the fluidized bed height to a step change or a sinusoidally varying fluidizing velocity may be considered as a first order (time-constant) system. This presupposes of course that the disturbance encountered will be small.

3. The development of the linearized model has led to a theoretical expression for the time constant as given by Equation (17) or (18).
4. Comparison of the calculated response with experimental results show that the limitation of the linearized model to small step inputs is not reflected in deviations of the calculated time constants. It is seen, however, that the size of input affects the time interval over which the theoretical model is applicable.
5. The pulse testing method of obtaining frequency response data is not generally useful in the analysis of bed height relationships in fluidized beds. It is recognized, however, that some useful results might be obtained by using a more efficient pulse form than the rectangular pulse.
6. It may be possible to treat aggregative fluidization in the same manner as particulate fluidization in determining transient bed height behavior. It is, however, necessary to use the values of U_s and n to calculate the time constant for this type of system even though they are not the experimental parameters of the steady-state relationship. This makes the procedure questionable.
7. Application of a sinusoidal input to a fluidized system will cause a shift in the steady-state height of the bed and a small amount of distortion can be expected in the output wave form.

8. Particle size distribution seems to have a definite effect on the dynamic behavior of fluidized beds.

ACKNOWLEDGMENT

The author wishes to express his sincere appreciation to Dr. Liang-tseng Fan, for his advice, patience, and guidance throughout this work; Dr. William H. Honstead, Head of the Department of Chemical Engineering for his interest and encouragement; Mr. Eugene N. Miller for help in reading and correcting the manuscript; and the National Science Foundation for partially supporting this project.

LITERATURE CITED

1. Wilhelm, R. H., and Kwauk, M., Chem. Engr. Prog., 44, 201 (1948).

2. Leva, Max, Fluidization, Mc-Graw Hill, 1959.

3. Ceaglske, N. H., Automatic Process Control for Chem. Engrs., John Wiley and Sons, (1956).

4. Richardson, J. F., and Zaki, W. N., "Sedimentation and Fluidization: Part I", Trans. Instn. Chem. Engrs. Vol. 32, (1954).

5. Slis, P. L., Willemse, Th. W., and Kramers, H., Applied Sci. Res., 8A, 209 (1959).

6. Hougen, J. O., and Walsh, R. A., Chem. Eng. Prog., 57, No. 3, 69 (1961).

7. Huss, Carol R. and Donegan, James J., National Advisory Committee for Aeronautics Technical Note NACA 3598 (January 1956).

8. Martin Nuclear Company, Technical Report MND-FBR-1696, (1959).

9. Kelly, V. P., Government Report HW-54991.

10. Foss, A. S., Symposium Series, Reactor Kinetics and Unit Operations, No. 25, Vol. 55, 47 (1959).

NOMENCLATURE

A = maximum bed expansion (step height), cm.

a = constant in Equation (65), cm./sec.

A_{col} = cross-sectional area of column, cm.^{2}.

A_{cy} = cross-sectional area of cylinder on sine wave generator. cm.^{2}.

B = slope of linear input of height variable, cm./sec.

b = constant in Equation (65), dimensionless.

D_p = diameter of particle, cm.

h = bed height at time, t, cm.

h_{ss} = steady-state bed height, cm.

h^* = input amplitude in bed height for frequency response, cm.

k = constant in Equation (57), sec.$^{-1}$.

L = length of lever arm on sine wave generator, cm.

n = constant in Equation (1), dimensionless.

N_{Re} = Reynolds number, dimensionless.

r_n = height of staircase function, cm.

t = time, sec.

$t_{0.02}$ = time interval defined by Equation (34), sec.

T = theoretical time constant, sec.

U_s = terminal falling velocity of particles, cm./sec.

V = volumetric flow rate, ml./sec.

V_L = tangential velocity of lever arm on sine wave generator, cm./sec.

V_s = velocity of piston in sine wave generator, cm./sec.

Greek Letters

α = phase lag, degrees.

ω = frequency, 1/sec.

ϵ = porosity, dimensionless.

ϵ_{ss} = steady-state porosity, dimensionless.

ϵ_h = porosity at top of bed, dimensionless.

ϕ = superficial liquid velocity, cm./sec.

ϕ_{ss} = steady-state superficial liquid velocity, cm./sec.

ϕ_1 = steady-state superficial liquid velocity after step input, cm./sec.

ϕ^* = amplitude of sine input in terms of superficial velocity, cm./sec.

ρ_L = density of liquid.

ρ_s = density of solid.

μ = viscosity of fluid.

APPENDIX

A. Bibliographical Essay

At the present time the need for experimental and theoretical studies in chemical process control is becoming increasingly apparent. In the past year there have been numerous technical publications on the response of chemical reactor systems to changes in composition and temperature. However, the pressure and flow fluctuation and their interactions with composition have not been treated. Without such information a complete analysis for the control of a process is impossible. (10) One example of such a process is the response of the liquid-solid fluidized bed to changes in fluidizing velocity.

The only experimental work in the transient behavior of fluidized beds to the authors knowledge was conducted by Slis, et. al. (5). Their work involved the development of a theoretical expression for the response of bed height to a step input in fluidizing velocity. Experimental results were presented to verify their equations.

As part of a study on the feasibility of fluidized bed nuclear reactors, Martin Nuclear Company (8) developed a differential equation to represent the transient behavior of bed height to changes in flow. This was a complicated, non-linear model and no solutions were obtained in analytical form. The model was programmed on the analog computer and responses obtained in this manner. No experimental work was conducted in their investigation, although the authors of the report recognized a need for such study and so stated at the end of their report.

It is evident then that work in this field has hardly begun, although there is a definite need for the information. Because of the interest in the use of fluidized beds as nuclear reactors as well as the present tendency toward more accurate process control, there will undoubtedly be more investigations of the transient behavior of fluidized beds in the near future.

B. Procedure for Application of Model

The following shows the manner in which the curve presented in Figure 19 was obtained. The problem is a hypothetical one which deals with an aspect of the feasibility of fluidized bed nuclear reactors. (8). The following data is given:

$\epsilon_{ss} = 0.700$

$h_{ss} = 5.0$ ft.

cross-sectional area bed = 3.48 ft^2.

bed diameter = 7.0 ft.

$\phi_{ss} = 1.40$ ft./sec.

$D_p = 0.205$ inches

bed weight = 63,021 pounds

temperature at bottom of bed = 472°F

temperature at top of bed = 574°F

ave. bed. temperature = 523°F

$\rho_f = 48.2$ lbs./$ft.^3$

$\rho_s = 624.1$ lbs./$ft.^3$

$U_s = 3.29$ ft./sec.

$\mu_f = 0.025$ cp. = 1.68×10^{-5} lbs./ft.-sec.

$$N_{Re} = \frac{\rho_f D_p U_s}{\mu_f} = \frac{(48.2)(0.205)(3.29)}{(12)(1.68)(10\text{-}5)} = 1.61 \times 10^5$$

Since N_{Re} is well over 500, from Equation (32)

$n = 2.39$

and the steady-state relationship should be

$$\phi_{ss} = U_s \epsilon_{ss}^{n} = 3.29\ \epsilon_{ss}^{2.39}$$

T is calculated from Equation (17) as

$$T = \frac{h_{ss}}{n U_s \epsilon_{ss}^{n-1}(1-\epsilon_{ss})} = \frac{(5)}{(2.39)(3.29)(0.700)^{1.39}(0.300)}$$

$$= 3.48 \text{ sec.}$$

or from Equation (18)

$$T = \frac{h_{ss}\epsilon_{ss}}{n\phi_{ss}(1-\epsilon_{ss})} = \frac{(5)(0.700)}{(2.39)(1.4)(0.300)}$$

$$= 3.48 \text{ sec.}$$

Now the steady-state relationship must be linearized about the point (ϕ_{ss}, ϵ_{ss}). An expression for the steady-state porosity is

$$\epsilon_{ss} = 1 - \frac{a}{h_{ss}}$$

where $a = \dfrac{\text{bed weight}}{\text{solid density} \times \text{cross-sectional area of column}} = \dfrac{(63.000)}{(624.1)(38.48)}$

$$= 2.63 \text{ ft.}$$

The steady-state relationship becomes

$$\phi_{ss} = U_s\left(1 - \frac{2.63}{h_{ss}}\right)^n$$

differentiation of this expression gives

$$\frac{d\phi_{ss}}{dh_{ss}} = n\,U_s\left(1 - \frac{2.63}{h_{ss}}\right)^{n-1}\left(\frac{2.63}{h_{ss}^2}\right)$$

which is evaluated at $h_{ss} = 5.0$ to give

$$\frac{d\phi_{ss}}{dh_{ss}} = (2.39)(3.29)\left(1 - \frac{2.63}{5.00}\right)^{1.39}\left(\frac{2.63}{25.0}\right) = 0.292 \text{ sec.}^{-1}$$

and we assume the straight line relationship

$$\frac{h_{ss}}{\phi_{ss}} = \frac{1}{0.292} = 3.43 \text{ sec.}$$

The first input to be considered is a linear flow input of 4.62×10^{-3} $\frac{\text{ft.}}{\text{sec.}}$/sec. Therefore the input in terms of bed height is

$$B = 3.43\,\phi = (3.43)(4.62)(10^{-3}) = 1.58 \times 10^{-2} \text{ ft./sec.}$$

and the input is to be of 27 second duration.

The differential equation giving the response to a linear input is

$$\frac{dh}{dt} + \frac{1}{T}h = \frac{Bt}{T}$$

which has the solution

$$h - h_{ss} = BT\left(e^{-\frac{t}{T}} + \frac{t}{T} - 1\right)$$

The following points are now calculated using the above equation.

t(sec.)	$h-h_{ss}$ (ft.)
5	3.66×10^{-2}
10	1.06×10^{-1}
15	1.83×10^{-1}
20	2.61×10^{-1}
25	3.40×10^{-1}
27	3.72×10^{-1}

At this point the input is to remain constant at (27 sec.)(1.58) (10^{-2}) ft./sec. = 0.426 ft. for 10 seconds. The response for this portion of the curve will be

$$h - h_{ss} = h\,u(t-27) - e^{-\frac{(t-27)}{T}} + 3.72 \times 10^{-1}$$

$$h = 0.426 - 0.372 = 0.044 \text{ ft.}$$

t(sec.)	$h-h_{ss}$ (ft.)
30	3.97×10^{-1}
35	4.12×10^{-1}
37	4.14×10^{-1}

Now there is to be a negative linear input with $B = 1.58 \times 10^{-2}$ ft./sec.

$$h - h_{ss} = BT\,u(t-37)\; e^{-\frac{(t-37)}{T}} + \frac{(t-37)}{T} - 1 + 0.414$$

This input is to be of 13.5 sec. duration. Calculated values are

t(sec.)	$h - h_{ss}$ (ft.)
40	3.98×10^{-1}
45	3.36×10^{-1}
50	2.62×10^{-1}
50-5	2.54×10^{-1}

Finally the input is to be constant at 0.213 ft.

$$h - h_{ss} = (0.213-0.254)\, u(t-50-5)-e^{-\frac{(t-50.5)}{T}} + 0.254$$

t(sec.)	$h - h_{ss}$ (ft.)
55	2.24×10^{-1}
60	2.16×10^{-1}
65	2.14×10^{-1}
70	2.13×10^{-1}

All of the response calculations shown here are plotted on Figure 19.

C. Outline of Proposed Research Project

The following are some suggestions concerning further research in the area of transient behavior of fluidized beds and related areas.

1. There is need for more work in the same area as this present work. In particular, the author would suggest that additional work be done on liquid-solid, particulate fluidization using experimental apparatus with a greater range than the apparatus used here. If a sine-wave generator were constructed so that the frequency-range was at least zero to two radians per second, considerable additional data could be obtained on phase lag and

amplitude ratio relationships with frequency. Also the use of moving pictures would provide an extremely accurate, but relatively expensive method of analysis. One of the better methods of following bed height is presented by Slis, et. al. (5). They used a follow-up system consisting of a traveling photoelectric tube and a vertical fluorescent lamp.

2. The dynamics of a single particle suspended in a flowing stream is possible. To accomplish this a column at least 4 inches in diameter should be employed for the study of small particles. The same function generating elements that were used in the fluidization study would be required. The particle could be suspended by using a steady-state flow equal to its terminal settling velocity. The flow could be changed in various ways and the motion of the particle observed. It is not known if there would be any practical value for such work, but it is possible that some information concerning basic particle dynamics could be gained.

3. A study of the effect of particle distribution on the transient behavior of fluidized beds is recommended. Several distributions could be used and the results compared. This would also involve a fairly extensive study of the steady-state axial distribution of particle diameter.

4. A study of the transient behavior of semi-fluidized beds would be useful. Semi-fluidization is becoming a very

popular process and there will surely be a need for work in this field.

DYNAMICS OF LIQUID-SOLID FLUIDIZED BED EXPANSION

by

JAMES ALBERT SCHMITZ

B. S., Kansas State University, 1959

AN ABSTRACT OF A THESIS

submitted in partial fulfillment of the

requirements for the degree

MASTER OF SCIENCE

Department of Chemical Engineering

KANSAS STATE UNIVERSITY
Manhattan, Kansas

1962

The dynamic response of bed height in liquid-solid fluidized beds to a change in fluidizing velocity was investigated. This system is recognized as a very non-ideal system from the standpoint of dynamic analysis. Not only is the system decidedly nonlinear, but different mechanisms for bed expansion and contraction are evident.

The problem was approached from such a direction as to lead to information useful in the control of fluidized processes. With this view in mind a linearized model was developed which could be expected to represent the response of fluidized bed height to small disturbances. The model developed was linear and first order expressed as:

$$\frac{dh}{dt} + \frac{h}{T} = \frac{h_1(t)}{T}$$

where h is the instantaneous bed height, h_1 is the input function in terms of bed height, and t is the time. Expressions were developed such that the time constant, T, for the system could be estimated using the parameters characterizing the system:

$$\frac{h_{ss}}{nU_s \epsilon_{ss}^{n-1}(1-\epsilon_{ss})} \qquad \frac{h_{ss}\,\epsilon_{ss}}{n\,\phi_{ss}\,(1-\epsilon_{ss})}$$

where h_{ss} is the steady-state bed height, n is a constant dependent on Reynolds number, U_s is the terminal falling velocity of the particles, ϵ_{ss} is the steady-state porosity, and ϕ_{ss} is the

steady-state superficial fluid velocity.

Experimental work was conducted to verify the linearized model. The inputs considered were step, pulse, and sinusoidal inputs in fluidizing velocity. The agreement of the linearized model with the experimental results was generally quite good for each of these inputs.

The response to a step-up in fluidizing velocity was represented much more accurately by the linearized model than the response to a step-down. This was because of the tendency of the bed height to give a linear response with time in the case of a step-down. Based on these considerations the time interval over which the linearized model could be expected to give an arbitrary degree of accuracy was defined.

An attempt was made to obtain frequency response data from the response to a pulse input by an approximating Fourier transform method. It was found that this technique could not be depended on to give meaningful results when applied in this investigation.

The results of frequency response analysis showed that the distortion appearing in the output wave due to non-linearity of the system was not severe for small input amplitudes. In this same analysis a shift in the steady-state bed height was observed when a sinusoidal input was applied.

It is proposed that particle size distribution may have a significant effect on the transient behavior of fluidization processes.

It was found that it is possible to treat the dynamic response of aggregative fluidized beds in much the same manner as particulate fluidization was treated in this work.

Transport and rate processes which are commonly carried out in fluidized beds are related to the porosity of the bed. Therefore, no study of such a process would be complete without taking into account the dynamic behavior of porosity or bed height.